NASA TECHNICAL MEMORANDUM

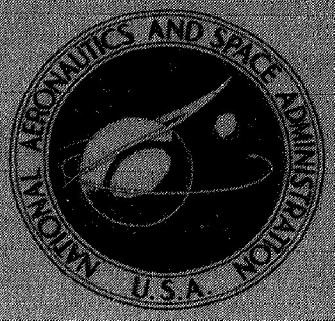

NASA TM X-1709

NASA TM X-1709

EXPERIMENTAL INVESTIGATION OF A 10° CONICAL TURBOJET PLUG NOZZLE WITH IRIS PRIMARY AND TRANSLATING SHROUD AT MACH NUMBERS FROM 0 TO 2.0

by Donald L. Bresnahan

Lewis Research Center
Cleveland, Ohio

NATIONAL AERONAUTICS AND SPACE ADMINISTRATION • WASHINGTON, D. C. • DECEMBER 1968

NASA TM X-1709

EXPERIMENTAL INVESTIGATION OF A 10° CONICAL TURBOJET PLUG NOZZLE WITH IRIS PRIMARY AND TRANSLATING SHROUD AT MACH NUMBERS FROM 0 TO 2.0

By Donald L. Bresnahan

Lewis Research Center
Cleveland, Ohio

NATIONAL AERONAUTICS AND SPACE ADMINISTRATION

For sale by the Clearinghouse for Federal Scientific and Technical Information
Springfield, Virginia 22151 – CFSTI price $3.00

ABSTRACT

The efficiency of a full-length plug nozzle with a simulated iris primary throat remained above 96.5 percent at all flight conditions except subsonic cruise where external flow effects were significant. Nozzle efficiency was also sensitive to subsonic cruise pressure ratio, varying from 0.918 to 0.942 for pressure ratios from 3.25 to 4.0. Plug truncations to 30 percent of full length at supersonic cruise resulted in a 1-percent loss in efficiency. At subsonic cruise, the effects of truncation were greater, resulting in approximately 1/2-percent efficiency loss with a 65-percent plug and more than 3-percent loss with the 30-percent plug length.

EXPERIMENTAL INVESTIGATION OF A 10° CONICAL TURBOJET PLUG NOZZLE WITH IRIS PRIMARY AND TRANSLATING SHROUD AT MACH NUMBERS FROM 0 TO 2.0

by Donald L. Bresnahan

Lewis Research Center

SUMMARY

An experimental investigation was conducted in the Lewis Research Center's nozzle static test facility and the 8 by 6 foot supersonic wind tunnel to determine the performance characteristics of a 10^{o} half-angle conical turbojet plug nozzle with a simulated iris primary throat and overall design pressure ratio of 26.3. The internal expansion of the nozzle was adjusted by translating a cylindrical outer shroud.

The efficiency of a full-length plug nozzle remained above 96.5 percent for all flight conditions except for subsonic cruise at Mach 0.9. At subsonic cruise, the external flow effects were greatest because the nozzle was operating at a low pressure ratio where the external drag became a large percent of the relatively low ideal thrust. Increasing the pressure ratio from 3.25 to 4.0 increased subsonic cruise efficiency from 0.918 to 0.942.

Truncating the plug to 30 percent of full length at supersonic cruise resulted in a 1-percent loss in efficiency. At subsonic cruise, however, the effects of truncation were greater, resulting in approximately a 1/2-percent efficiency loss with the 65-percent plug and more than 3-percent loss for the 30-percent plug length.

The pumping characteristics of the nozzle indicate that secondary flow could be provided to cool the primary nozzle and the shroud at all flight conditions except takeoff. In general, optimum thrust performance was obtained with 4- to 6-percent corrected secondary flow ratio.

INTRODUCTION

As part of a broad program in airbreathing propulsion, the Lewis Research Center is evaluating various nozzle geometries appropriate for supersonic cruise applications. In this continuing program, plug nozzles are receiving considerable emphasis because they

may offer the potential of good aerodynamic performance together with a minimum of complexity and a consequent reduction in maintenance problems. This report documents the aerodynamic performance of a plug nozzle configuration suitable for an afterburning turbojet engine designed for cruise at a Mach number near 2.7.

High internal performance can be obtained with isentropic plug nozzles. External flow, however, has an adverse effect on performance of this type of nozzle due to the high base drag and resultant over-expansion losses on the plug surface at off-design pressure ratios resulting from the high lip angles inherent with this design (refs. 1 to 3). Another approach to plug nozzle design is the low angle conical plug with a small boattail angle (ref. 4). This nozzle reduces the base drag and overexpansion effects by reducing the boattail angle. Good subsonic performance is obtained, but for transonic and supersonic operation it must incorporate a translating shroud to provide internal expansion appropriate for the particular Mach number and its corresponding pressure ratio. Plug nozzle with translating shrouds were studied (ref. 5) for overall design pressure ratios up to 20 and plug half angles of $7\frac{1}{2}^{\circ}$, 10°, and 15°. It was determined a 10° half angle was optimum; however, the variations in pressure ratio and Mach number were rather limited. In practice, the shroud would translate to keep the internal expansion pressure ratio approximately equal to the nozzle pressure ratio. However, the maximum shroud length was determined by the condition at which the initial Mach line from the shroud lip just intercepted the plug tip. At higher pressure ratios, the shroud remains fixed since any further extension adds weight and friction without affecting the plug expansion field. This limiting internal expansion pressure ratio varies with both plug angle and nozzle design pressure ratio. For the 10° half-angle plug of reference 5, this ratio was approximately 80 percent of the nozzle design pressure ratio. To determine the performance of a nozzle with a higher design pressure ratio, a fixed-throat nozzle with a 10° half-angle plug and translating shroud and an overall design pressure ratio of 26.3 was tested at Mach numbers up to 2.0 (ref. 6). The performance could be maintained at a high level by extending the shroud with increases in nozzle pressure ratio from 2.5 to 30.

To provide for changes in engine-operating conditions, such as an afterburner, the nozzle should have a variable throat. The present investigation was conducted to determine the performance of a plug nozzle with a fixed centerbody and simulated iris-type primary flaps for throat area modulation. A 10° half-angle plug nozzle with a translating external cylindrical shroud and an overall design pressure ratio of 26.3 was tested in the Lewis Research Center's nozzle static test facility to investigate quiescent performance and also in the 8 by 6 foot supersonic wind tunnel at Mach numbers up to 1.97 to determine the external flow effects. Variations in shroud cooling flow rates of up to 20-percen corrected secondary flow ratio were studied to determine the effect on performance. Plu truncation to approximately two-thirds, one-half, and one-third of the original length wer

also studied. Dry air at room temperature was used for primary and secondary flows in both facilities and maximum nozzle pressure ratios of 30.0 were obtained.

SYMBOLS

A	area
D	drag
d	model diameter
F	thrust
l	full plug length measured from nozzle throat
M	Mach number
P	total pressure
p	static pressure
r	radius
T	total temperature
w	weight flow rate
x	axial distance measured from nozzle throat
θ	circumferential position

Subscripts:

bt	boattail
i	ideal
j	jet
max	maximum
p	primary
s	secondary
x	condition at distance x
0	free stream
7	nozzle inlet
8	nozzle throat
9	nozzle exit

APPARATUS AND INSTRUMENTATION

Installation in Static Test Facility

A schematic view and photograph of the research hardware installation in the static test facility is shown in figures 1 and 2. The nozzles were mounted on a section of pipe which was freely suspended by four flexure rods connected to the bedplate. Pressure forces acting on the nozzle and mounting pipe, both external and internal, were transmitted from the bedplate through a bell crank to a calibrated balanced-air-pressure diaphragm which was used in measuring thrust. A labyrinth seal around the necked-down inlet section ahead of the mounting pipe separated the nozzle-inlet air from the exhaust and provided a means of maintaining a pressure difference across the nozzle. The space between the two labyrinth seals was vented to the test chamber. This decreased the pressure differential across the second labyrinth and prevented a pressure gradient on the outside of the diffuser section due to an air blast from under the labyrinth seal.

Pressures and temperatures were measured at the various stations indicated. Total and wall static pressure measurements were used at the bellmouth inlet to compute inlet momentum, and at the primary air-metering station to compute the primary airflow. The nozzle-inlet total pressure and temperature were measured at station 7 and ambient exhaust pressure at station 0.

Installation in 8 by 6 Foot Supersonic Wind Tunnel

A schematic drawing of the model support system in the 8 by 6 foot supersonic wind tunnel showing the internal geometry and thrust-measuring system is shown in figure 3, with a photograph of the model installation in figure 4. The grounded portion of the model was supported from the tunnel ceiling by a vertical strut. The floating portion was attached to the primary and secondary air bottles cantilevered by flow tubes from external supply manifolds. The primary air bottle was supported by front and rear bearings. The secondary air passed through hollow struts at station 100.66 (255.68 cm) to the annulus formed between the primary nozzle and the shroud. The axial force of the nozzle, which included secondary flow effects, was transmitted to the load cell located in the nose of the model. Since the floating portion of the model included a portion of the afterbody and boattail, the measured force was that resulting from the interaction of the internal and external flows of the nozzle.

A static calibration of the thrust-measuring system was obtained by applying known forces to the nozzle and measuring the output of the load cell. A water-cooled jacket surrounded the load cell and maintained a constant temperature of 90° F (305.6 K) to elimi-

nate errors in the calibration due to variations in temperature from aerodynamic heating.

Nozzle Configurations

The nozzle configurations consisted of a 10° half-angle plug with shrouds of varying lengths to simulate translation. Its overall design pressure ratio was 26.3. Basic nozzle dimensions are shown in figure 5(a). The maximum model diameter was 8.5 inches (21.59 cm) with a circular arc boattail on the shroud to reduce base drag. The shroud base area ratio A_{bt}/A_{max} was arbitrarily selected to be 0.1146. In figure 5(b) are shown the shroud extensions that were tested, and their corresponding design pressure ratios and internal area ratios are listed in table I.

The plug was fabricated with several aft sections as shown in figure 5(c) to study the effect of plug truncation on nozzle performance. Due to the limitation of the number of separate air supplies in the test facilities, base bleed effects could not be studied; therefore, the plugs had solid bases.

The simulated iris-type primary flaps consisted of two fixed-geometry primary nozzles with a $17^{\circ}30'$ boattail (afterburner off) and a $7^{\circ}36'$ boattail (afterburner on) providing a 40-percent change in throat area, as shown in figure 6.

Nozzle Instrumentation

The primary and secondary total pressures were obtained by use of total pressure probes as shown in figure 7(a). The primary rake was area weighted. A row of static pressure orifices was located on the plug at a meridian angle of 180° (fig. 7(b)) with some orifices also located at angles of 0° and 270°.

PROCEDURE

Static Test Facility

Pressure ratios were set by maintaining a constant nozzle-inlet pressure and varying the exhaust pressure. Each configuration was tested over a range of pressure ratios which were appropriate for the particular shroud extension ratio.

8 by 6 Foot Supersonic Wind Tunnel

Nozzle performance was obtained over a range of pressure ratios at several Mach numbers for each shroud length tested. Since tunnel static pressure was fixed at a given Mach number, the nozzle pressure ratio was varied by changing the nozzle-inlet pressure. The maximum pressure ratio at each Mach number was restricted due to the limitations of the primary air supply. The highest pressure ratio obtained was approximately 27.0 at Mach 1.97. To obtain a realistic simulation of important flight conditions, nozzle pressure ratio was varied at each Mach number around a typical schedule for a supersonic turbojet engine which is shown in figure 8.

DATA REDUCTION

Static Test Facility

The nozzle primary airflow was calculated from pressure and temperature measurements in the necked-down section of the mounting pipe and an effective area determined by an ASME calibration nozzle. The secondary airflow was measured by means of a standard ASME flow-metering orifice in the external supply line.

Actual jet thrust was calculated from thrust-cell measurements corrected for tare forces. The ideal jet thrust for each of the primary and secondary flows was calculated from the measured mass flow rate expanded from their measured total pressures to p_0. Provision was made to equate the ideal thrust of the secondary flow to zero if the total pressure was less than p_0. Data where this condition existed are identified on the curves. Nozzle efficiency is defined then as the ratio of the actual jet thrust to the ideal thrust of both primary and secondary flows:

$$\text{Nozzle static efficiency} = \frac{F_j}{F_{ip} + F_{is}}$$

8 by 6 Foot Supersonic Wind Tunnel

Both primary and secondary flow rates were measured by means of standard ASME flow-metering orifices located in the external supply lines. Thrust-minus-drag measurements were obtained from a load cell readout of the axial forces acting on the floating portion of the model. Internal tare forces, determined by internal areas and measured

tare pressures located as shown in figure 3, were accounted for in the thrust calculation.

The only external friction drag charged to the nozzle is that downstream of station 113.49 (288.3 cm), shown in figure 3. That force acting on the portion of the nozzle between station 93.65 (237.9 cm) and 113.49 (288.3 cm) was also measured on the load cell, but it is not considered to be part of the nozzle drag. Its magnitude was estimated using the semi-empirical flat-plate mean skin friction coefficient given in figure 7 of reference 7 as a function of free-stream Mach number and Reynolds number. The coefficient accounts for variations in boundary-layer thickness and profile with Reynolds number. Previous measurements of the boundary layer characteristics at the aft end of this jet exit model in the 8 by 6 foot supersonic wind tunnel indicated that the profile and thickness were essentially the same as that computed for a flat plate of equal length. The strut wake appeared to affect only a localized region near the top of the model and resulted in a slightly lower local free-stream velocity than measured on the side and bottom of the model. Therefore, the results of reference 7 were used without correction for three-dimensional flow effects or strut interference effects. The resulting correction was applied to the load cell force.

The ideal jet thrust for each of the primary and secondary flows was calculated from the measured mass flow rate expanded from their measured total pressures to p_0. Provision was made to equate the ideal thrust of the secondary flow to zero if the total pressure was less than p_0. Data where this condition exists are identified on the curves. Nozzle efficiency is defined then as the ratio of the thrust-minus-drag to the ideal thrust of both primary and secondary flows:

$$\text{Nozzle efficiency} = \frac{F - D}{F_{ip} + F_{is}}$$

RESULTS AND DISCUSSION

Full-Length Plug

The full-length plug nozzle was tested with shrouds of varying length to simulate translation, and two primary nozzles simulating iris-type throat flaps for afterburner on and off operation. Each configuration was tested over a range of nozzle pressure ratios and Mach numbers corresponding to a typical schedule for a supersonic turbojet engine.

Afterburner on. - The afterburner-on configuration with a full-length plug and three shroud positions to simulate shroud translation during transonic and supersonic acceleration is shown in figure 9. These configurations were tested over a wide range of pressure ratios and Mach numbers from takeoff to Mach 2.0. The performance of these con-

figurations without secondary flow is shown in figure 10, and with 4 percent corrected secondary flow ratio in figure 11. It can be seen that a high level of performance can be maintained over a wide range of pressure ratios and Mach numbers by extending the shroud with increases in nozzle pressure ratio.

In an attempt to minimize the drag induced by the internal base formed between the primary flap and the extended shroud, some secondary flow is necessary. It would also be required for shroud cooling purposes. With the shroud retracted, secondary flow would be discharged through the annular gap at the shoulder of the primary nozzle afterbody. The effect of secondary flow on nozzle performance is shown in figure 12. The only data shown here are for the Mach numbers at which the afterburner would be on. In general, peak performance occurred with 4 to 6 percent corrected secondary flow ratio.

Pumping characteristic curves are shown in figure 13. The pressure recovery needed to supply this secondary flow is shown in figure 14. At takeoff, with the shroud retracted, there is no pumping; as a result, any secondary flow would have to come from the engine cycle. With external flow, at the subsonic and supersonic speeds shown, the pumping is such that the 4- to 6-percent secondary flow ratio could be obtained from inlets. At the higher supersonic speeds, secondary flow ratios greater than 8 percent could be obtained.

External flow effects on plug pressure distributions are shown in figure 15 for selected pressure ratios and Mach numbers with the appropriate shroud position. There was good agreement between the two facilities at $M_0 = 0$. The external flow effects were negligible at most Mach numbers with the greatest effect occurring at Mach 1.20. This occurred on the last one-third of the plug where the projected area is small.

Afterburner off. - The afterburner-off configuration with a full-length plug and three shroud positions to simulate translation is shown in the photographs in figure 16. These configurations were tested over a wide range of pressure ratios and Mach numbers to include subsonic acceleration, and subsonic and supersonic cruise. The effect of external flow on performance of these configurations, without secondary flow, is shown in figure 17. The shroud location corresponding to 80-percent internal expansion is shown in figure 17(c). It can be seen that performance at the higher pressure ratios is not improved with further extension of the shroud (fig. 17(d)). This is due to the plug expansion field not being affected by further shroud extension once the initial Mach line from the shroud lip has passed the plug tip as discussed earlier.

Some secondary flow will also be necessary with the afterburner off; therefore, its effect on nozzle performance is shown in figure 18. With the exception of subsonic cruise, peak performance was obtained with 4- to 6-percent corrected secondary flow ratio. At subsonic cruise, however, performance continued to increase with corresponding increases in secondary flow.

Pumping characteristic curves are shown in figure 19 for the subsonic cruise and

supersonic cruise configurations. The pressure recovery needed to supply this secondary flow is shown in figure 20. There is some external flow effect which improves the pumping, especially at subsonic cruise where the shroud is fully retracted.

The effects of external flow on plug pressure distribution are shown in figure 21 for selected pressure ratios and Mach numbers for the shroud position giving the optimum performance. The effect is negligible except at subsonic cruise (fig. 21(d)) where it appears to be favorable due to the damped plug pressure distribution following the initial overexpansion. With external flow, the pressures remain near ambient after the initial overexpansion with the plug force accounting for 5.1 percent of the nozzle thrust. In quiescent air there are two additional overexpansions and the plug force only accounts for 2.1 percent of the nozzle thrust. This favorable effect of external flow is more than offset, however, by the skin friction and boattail drag, resulting in the greatest external flow effects at subsonic cruise.

A summary of the full-length plug nozzle performance at various Mach numbers from takeoff to supersonic cruise is shown in figure 22. Each point indicates the optimum performance of the shrouds tested based on the operating schedule of figure 8. The secondary flow rates indicated were based on anticipated cooling requirements. Static test data were used to determine both the supersonic cruise and takeoff performance where the external flow effects are negligible. The shroud was fully retracted for all the subsonic Mach numbers except for afterburner-on operation at Mach 0.9 where the intermediate shroud position gave slightly higher performance. For Mach numbers 1.2 and higher, the shroud was extended to the position corresponding to 80-percent internal expansion for optimum performance. The efficiency remained above 96.5 percent for all flight conditions shown except subsonic cruise.

The maximum external flow effects occurred at subsonic cruise where the performance is very sensitive to both pressure ratio and Mach number. The nozzle was operating at a low pressure ratio where the external drag became a large percent of the relatively low ideal thrust. As indicated on the figure, increasing the operating pressure ratio from 3.25 to 4.0 increased the efficiency from 0.918 to 0.942.

Truncated Plugs

There is a continuing effort to increase the payload or range of aircraft by increasing the performance or decreasing the weight of engine components. Plug nozzle weight reduction can be accomplished by shortening the plug if the performance penalty is not too great. Truncated plugs of 65, 50, and 30 percent of full length (as shown in fig. 23), therefore, were tested to determine the effect of truncation on the plug nozzle performance.

The performance of the 65-percent plug nozzle with the shroud retracted and without secondary flow at subsonic speeds is shown in figure 24. The effects of secondary flow on nozzle performance are shown in figure 25. With the exception of subsonic cruise ($M_0 = 0.9$, $P_7/p_0 = 3.25$) peak performance generally occurred with between 2 and 4 percent corrected secondary flow ratio.

The 50-percent plug nozzle performance without secondary flow at subsonic and supersonic speeds is shown in figure 26. Secondary flow effects on performance are shown in figure 27. Again peak performance occurs with 2- to 4-percent corrected secondary flow ratio with the exception of subsonic cruise and Mach 1.97. For the supersonic cruise performance, quiescent data were used because the external flow effects at Mach 2.7 are negligible. This performance is shown in figure 28 with 0- and 2-percent corrected secondary flow ratio over a range of pressure ratios. The effect of secondary flow ratio on nozzle performance at the supersonic cruise pressure ratio is shown in figure 29 with peak performance occurring at 4 percent.

In figure 30 is shown the performance of the 30-percent plug nozzle without secondary flow at subsonic Mach numbers. The effect of secondary flow is shown in figure 31. For the supersonic cruise performance, the quiescent data again were used. This performance is shown in figure 32 for both 0- and 2-percent corrected secondary flow ratio over a range of pressure ratios. The effect of secondary flow on performance at the supersonic cruise pressure ratio is shown in figure 33. Peak performance occurs near 2-percent corrected secondary flow ratio with little change at increased flow rates.

A summary of the truncated plug performance for supersonic cruise and subsonic cruise is shown in figure 34. At supersonic cruise with the extended shroud and high pressure ratio, the effects of truncation are not very great. There was approximately 1-percent loss in efficiency with the 30-percent plug length and just over 1/2-percent loss with the 50-percent truncation. At subsonic cruise with the shroud retracted and when operating at a low pressure ratio, the effect of truncating the plug is considerably greater. With the 65-percent plug length, there is approximately 1/2-percent loss in efficiency, and this loss increased to over 3 percent with the 30-percent plug.

Because of the limitation of air supplies in the test facilities as previously stated, the effect of base bleed on these truncated plugs could not be studied. Previous tests (ref. 6), however, show that small amounts of base bleed flow reduce the loss due to truncation. With $1\frac{1}{2}$-percent base bleed, approximately one-third to one-half of this loss was regained.

SUMMARY OF RESULTS

An experimental investigation was conducted to determine the external flow effects

on the performance characteristics of a 10° half-angle conical turbojet plug nozzle with a simulated iris-type variable throat and an overall design pressure ratio of 26.3. The internal expansion was adjusted by translating a cylindrical outer shroud. The following general trends were indicated:

1. The efficiency of a full-length plug nozzle remained above 96.5 percent from takeoff through subsonic and supersonic acceleration to supersonic cruise. At subsonic cruise, the external flow effects were greatest and nozzle performance was sensitive to pressure ratio. For example, increasing the pressure ratio from 3.25 to 4.0 increased subsonic cruise efficiency at Mach 0.9 from 0.918 to 0.942.

2. Truncating the plug to 30 percent of full length resulted in a 1-percent loss in efficiency at supersonic cruise. At subsonic cruise, however, the effects of truncation were greater, resulting in approximately 1/2-percent efficiency loss with the 65-percent plug and more then 3 percent with the 30-percent plug length.

3. The pumping characteristics of the nozzle were such that secondary flow could be provided to cool the primary nozzle and the shroud at all flight conditions except takeoff. In general, optimum thrust performance was obtained with about 4- to 6-percent corrected secondary flow ratio.

National Aeronautics and Space Administration,
Lewis Research Center,
Cleveland, Ohio, July 22, 1968,
126-15-02-10-22.

REFERENCES

1. Valerino, Alfred S.; Zappa, Robert F.; and Abdalla, Kaleel L.: Effects of External Stream on the Performance of Isentropic Plug-Type Nozzles at Mach Numbers of 2.0, 1.8, and 1.5. NASA Memo 2-17-59E, 1959.

2. Salmi, Reino J.: Preliminary Investigation of Methods to Increase Base Pressure of Plug Nozzles at Mach 0.9. NACA RM E56J05, 1956.

3. Salmi, R. J.; and Cortright, E. M., Jr.: Effects of External Stream Flow and Afterbody Variations on the Performance of a Plug Nozzle at High Subsonic Speeds. NACA RM E56F11a, 1956.

4. Schmeer, James W.; Kirkham, Frank S.; and Salters, Leland B., Jr.: Performance Characteristics of a 10° Conical Plug Nozzle at Mach Numbers Up to 1.29. NASA TM X-913, 1964.

5. Herbert, M. V.; Golesworthy, G. T.; and Herd, R. J.: The Performance of a Centre Body Propelling Nozzle With a Parallel Shroud in External Flow, Part II. Rep. ARC CP-894, Aeronautical Research Council, Great Britain, 1966.

6. Bresnahan, Donald L.; and Johns, Albert L.: Cold Flow Investigation of a Low Angle Turbojet Plug Nozzle With Fixed Throat and Translating Shroud at Mach Numbers From 0 to 2.0. NASA TM X-1619, 1968.

7. Smith, K. G.: Methods and Charts for Estimating Skin Friction Drag in Wind Tunnel Tests With Zero Heat Transfer. Rep ARC CP-824, Aeronautical Research Council, Great Britain, 1965. (Available from DDC as AD-487132.)

TABLE I. - SHROUD VARIABLES

[Overall design pressure ratio, 26.3.]

Shroud length to diameter ratio, x/d	Afterburner off		Afterburner on	
	Internal expansion pressure ratio, P_7/p_9	Internal area ratio, A_9/A_8	Internal expansion pressure ratio, P_7/p_9	Internal area ratio, A_9/A_8
-0.235	1.89	1.0	1.89	1.0
.215	16.06	2.54	8.87	1.81
.618	21.10	2.99	11.93	2.13
1.270	25.80	3.39	14.85	2.42

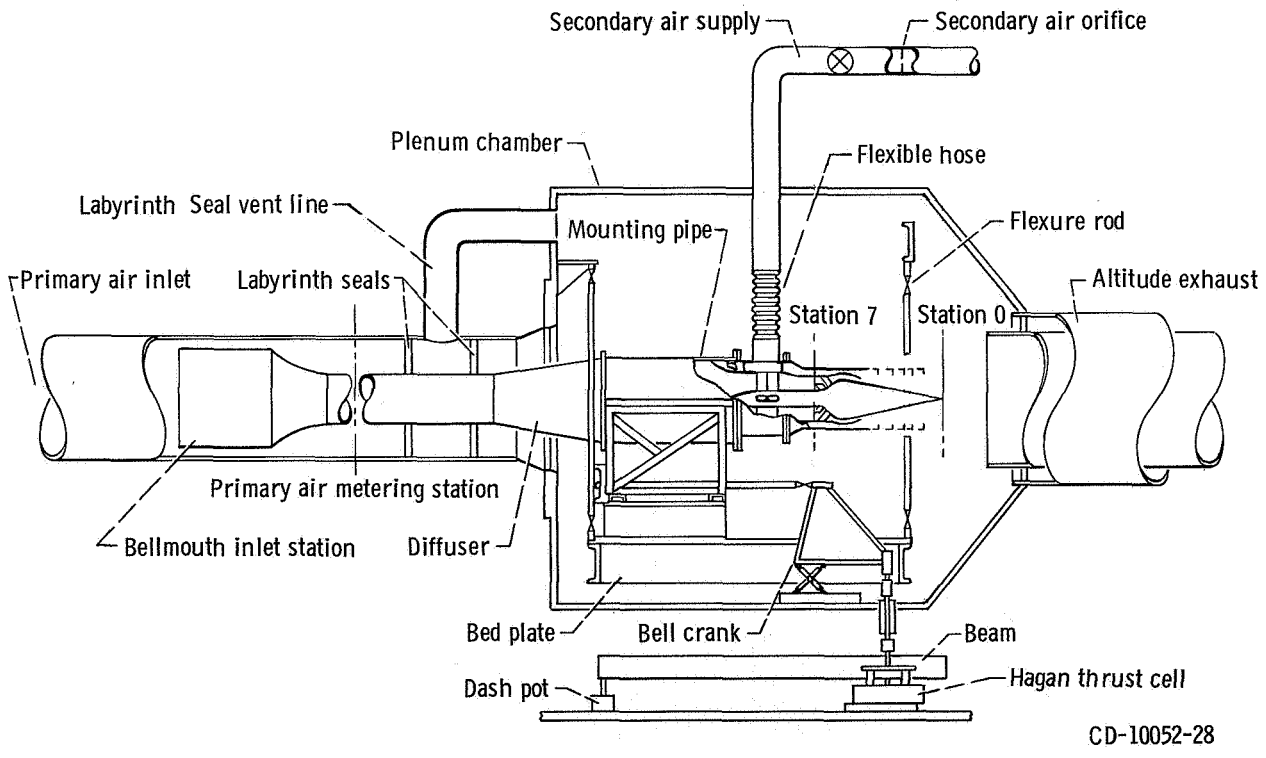

Figure 1. - Schematic view of static test stand.

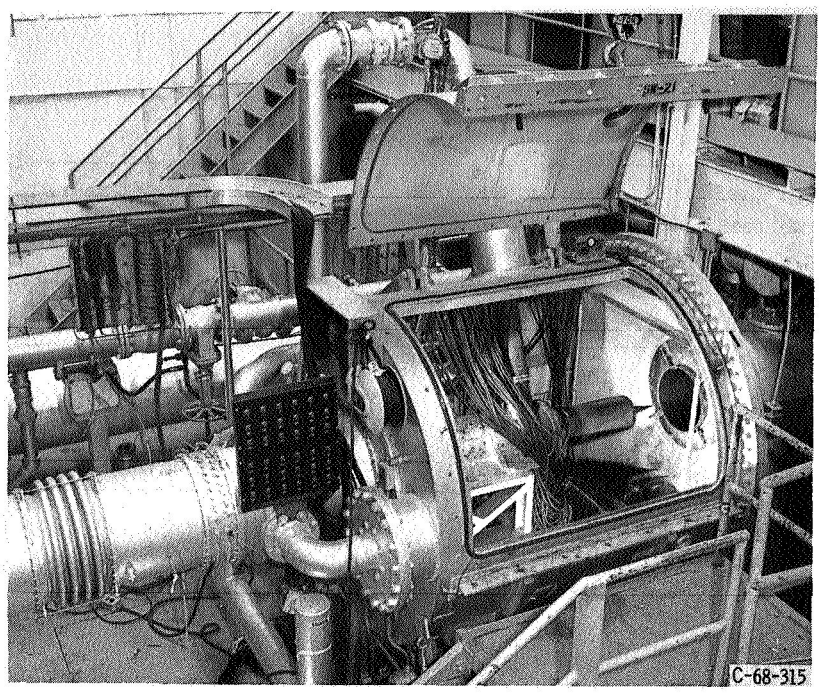

Figure 2. - Installation of nozzle in static test stand.

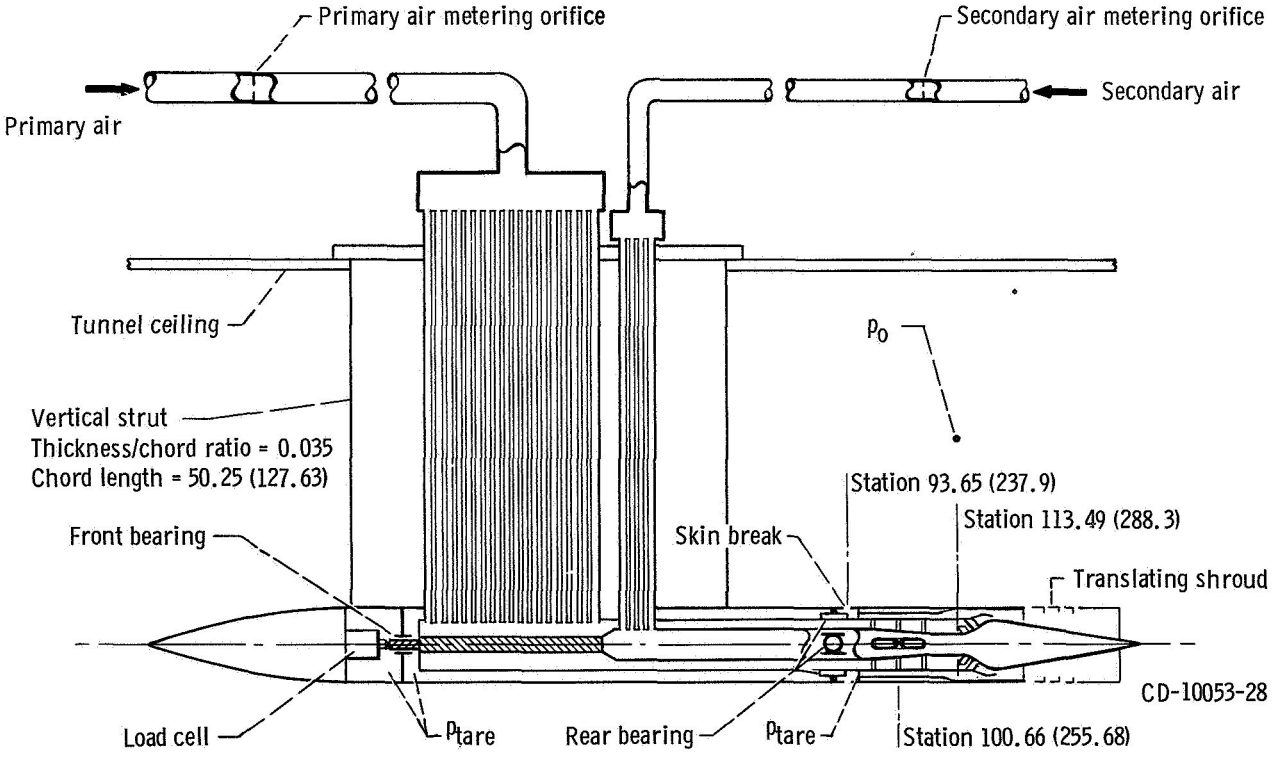

Figure 3. - Schematic view of nozzle support model and air supply systems for 8 by 6 foot supersonic wind tunnel. (All dimensions are in inches (cm).)

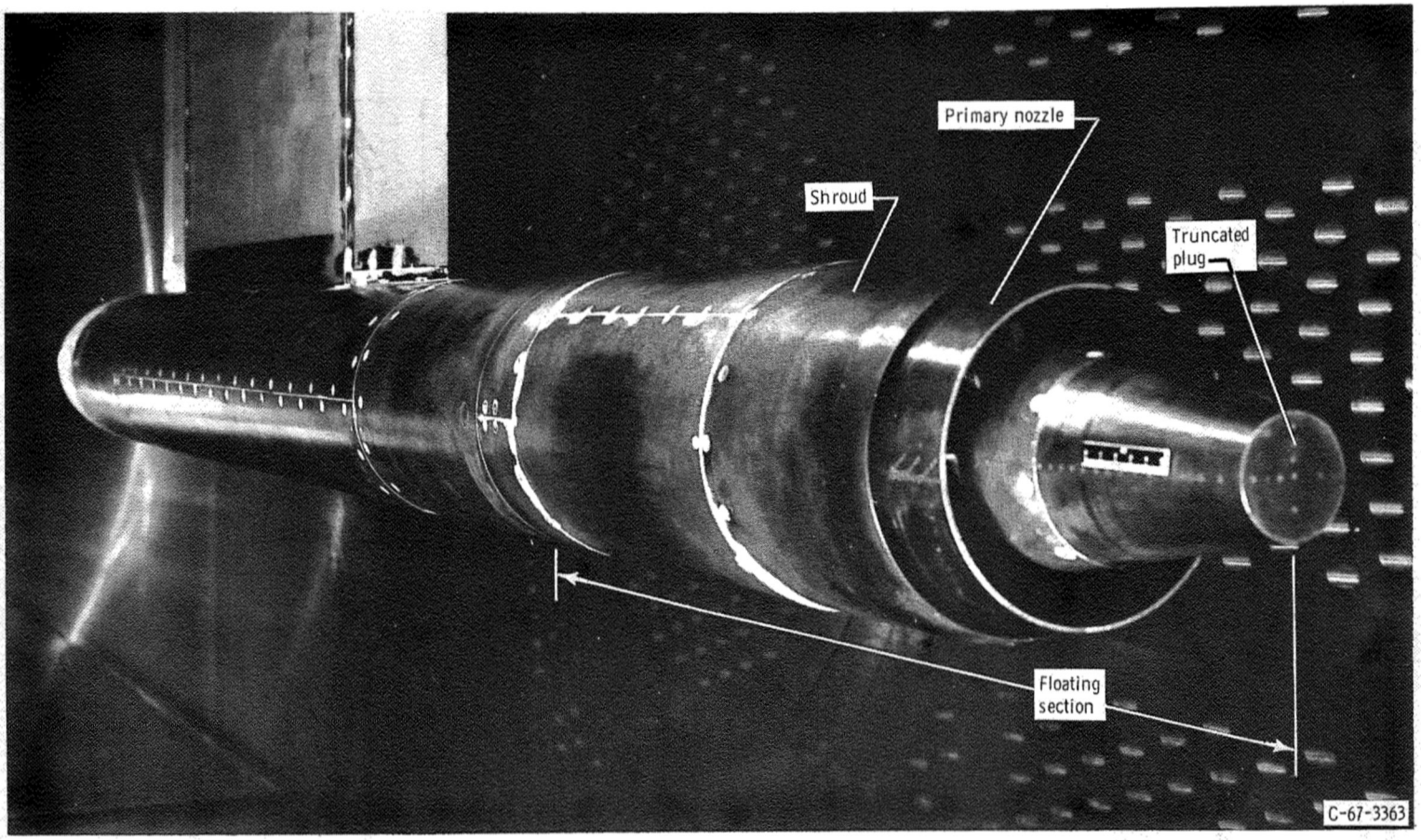

Figure 4. - Installation of nozzle in 8 by 6 foot supersonic wind tunnel.

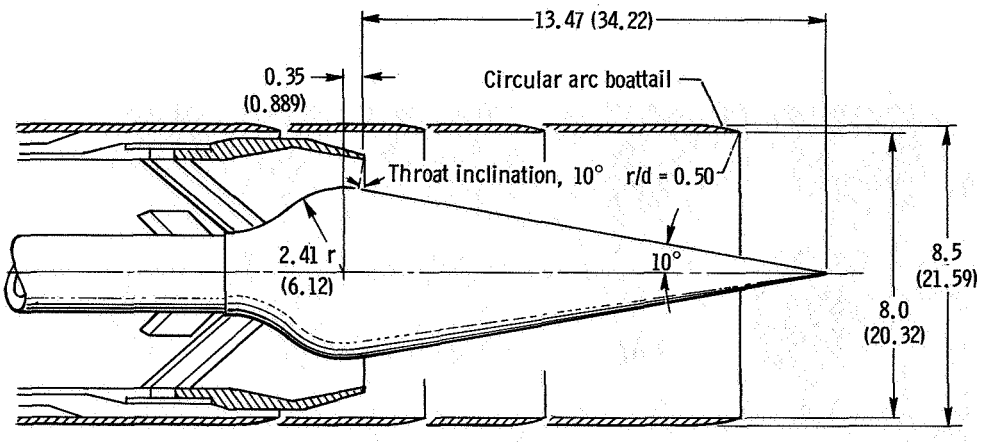

(a) Plug nozzle model dimensions.

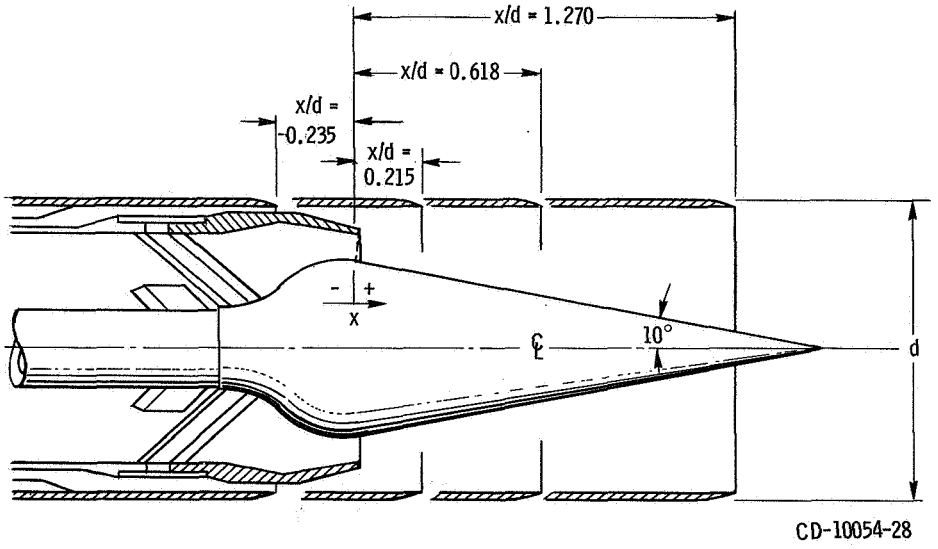

(b) Plug nozzle shroud locations.

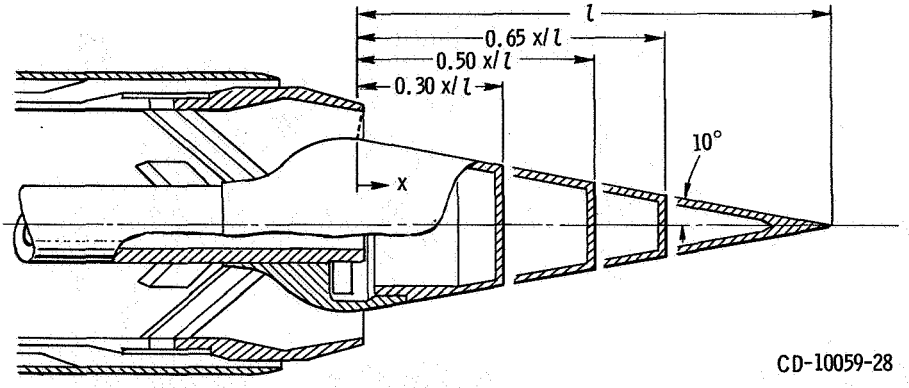

(c) Plug nozzle truncations.

Figure 5. - Model dimensions and geometric variables. (All dimensions are in inches (cm) unless otherwise noted.)

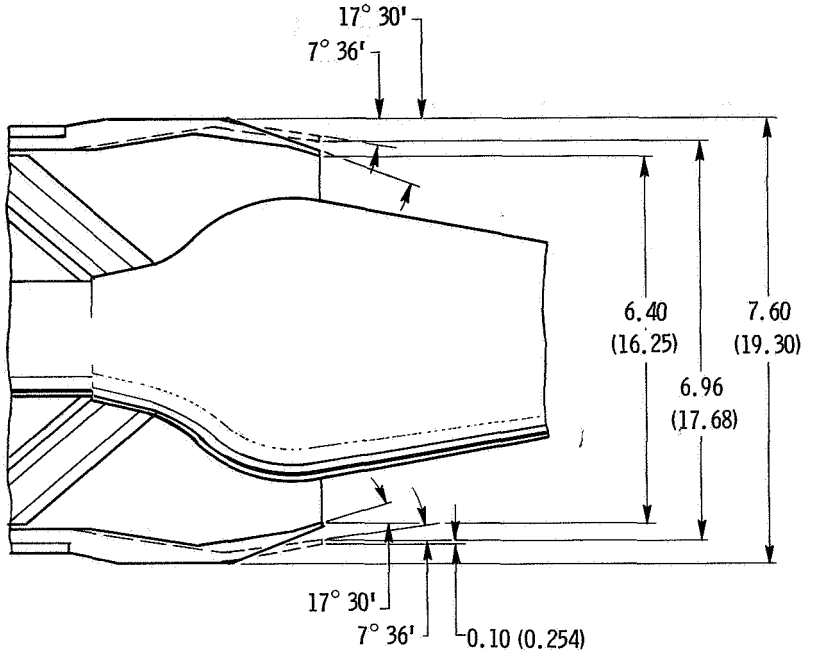

Figure 6. - Iris primary nozzle. (All dimensions are in inches (cm) unless otherwise noted.)

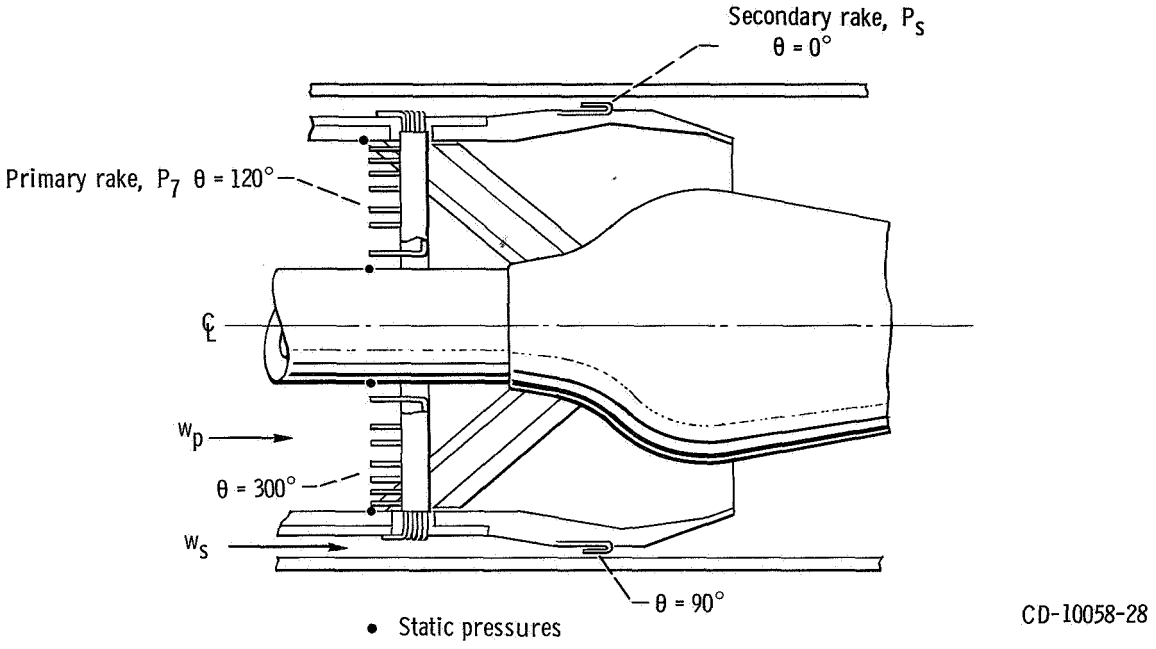

(a) Primary and secondary rakes.

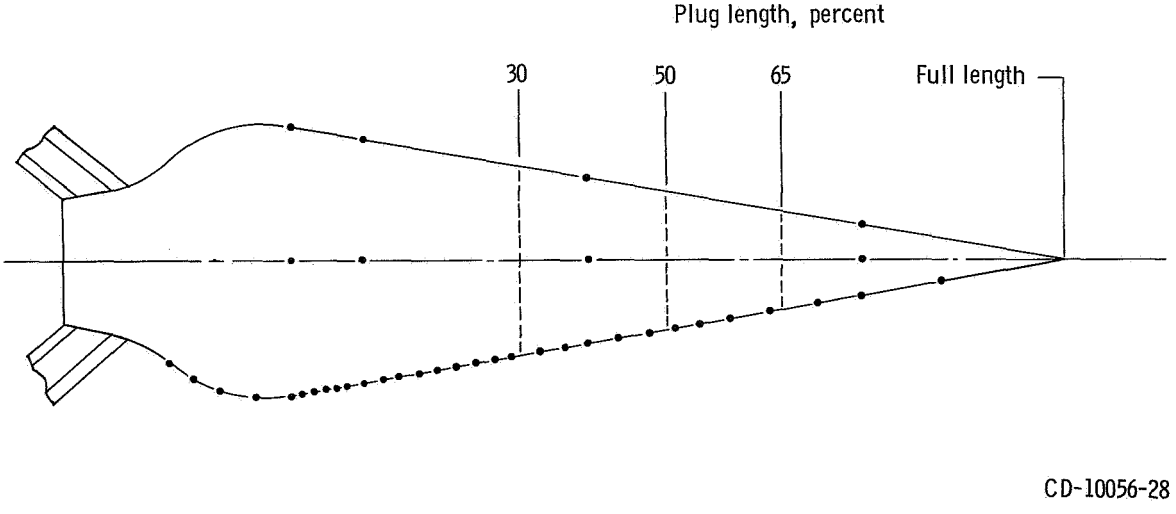

(b) Plug static pressure locations.

Figure 7. - Model Instrumentation.

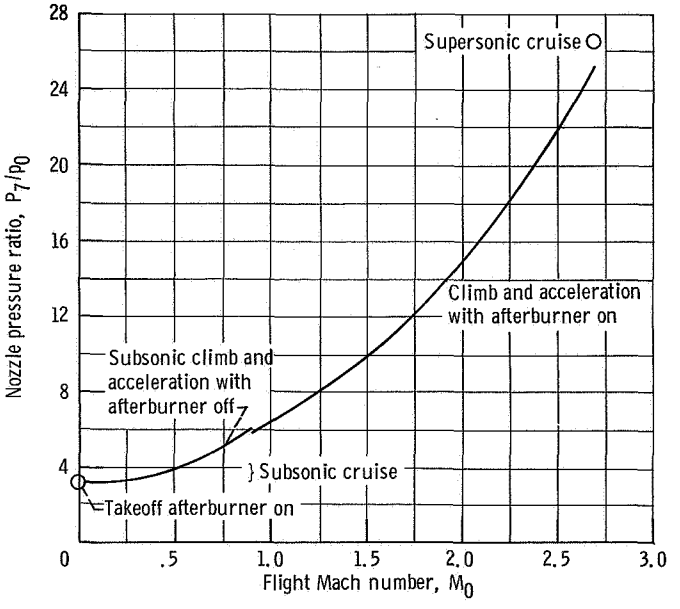

Figure 8. - Pressure ratio schedule for typical turbojet engine.

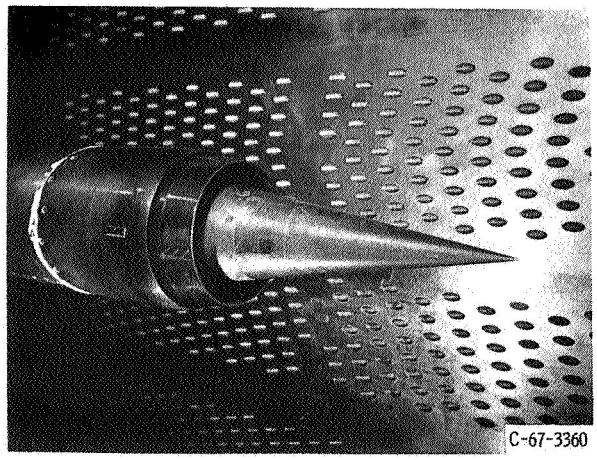

(a) Shroud length to diameter ratio, x/d = -0.235; internal area ratio, A_9/A_8 = 1.0.

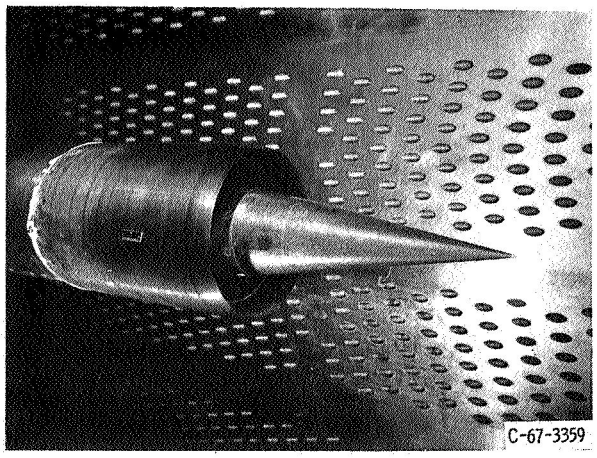

(b) Shroud length to diameter ratio, x/d = 0.215; internal area ratio, A_9/A_8 = 1.81.

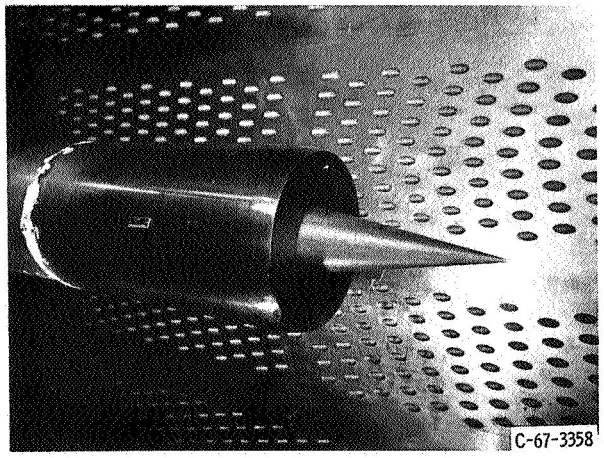

(c) Shroud length to diameter ratio, x/d = 0.618; internal area ratio, A_9/A_8 = 2.13.

Figure 9. - Full-length plug with translating shroud and afterburner on.

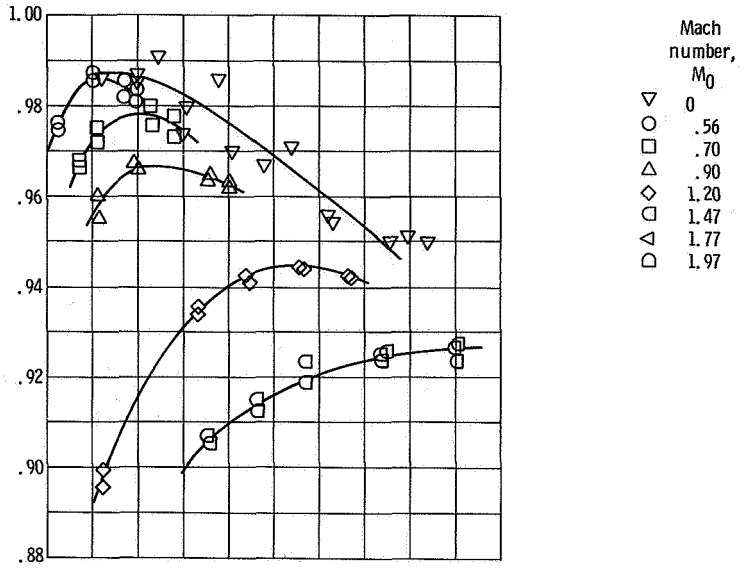

(a) Shroud length to diameter ratio, x/d = -0.235; internal area ratio, A_9/A_8 = 1.0.

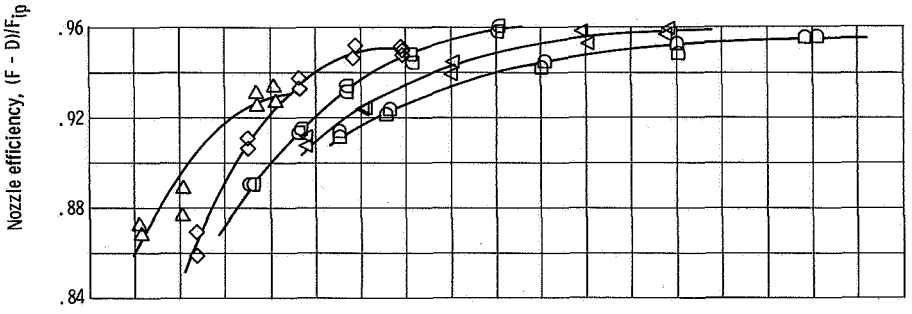

(b) Shroud length to diameter ratio, x/d = 0.215; internal area ratio, A_9/A_8 = 1.81.

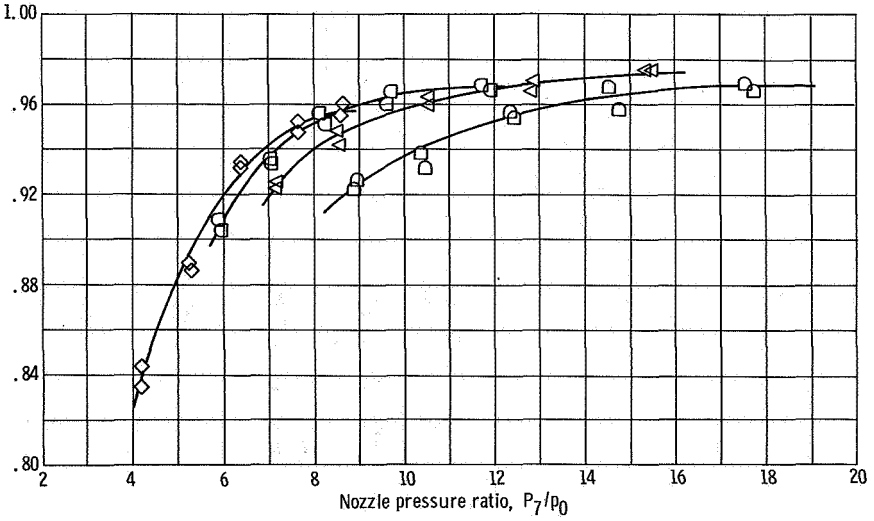

(c) Shroud length to diameter ratio, x/d = 0.618; internal area ratio, A_9/A_8 = 2.13.

Figure 10. - External flow effect on full-length plug nozzle performance; afterburner on; corrected secondary flow ratio, $(w_s/w_p)\sqrt{T_s/T_p}$ = 0 percent.

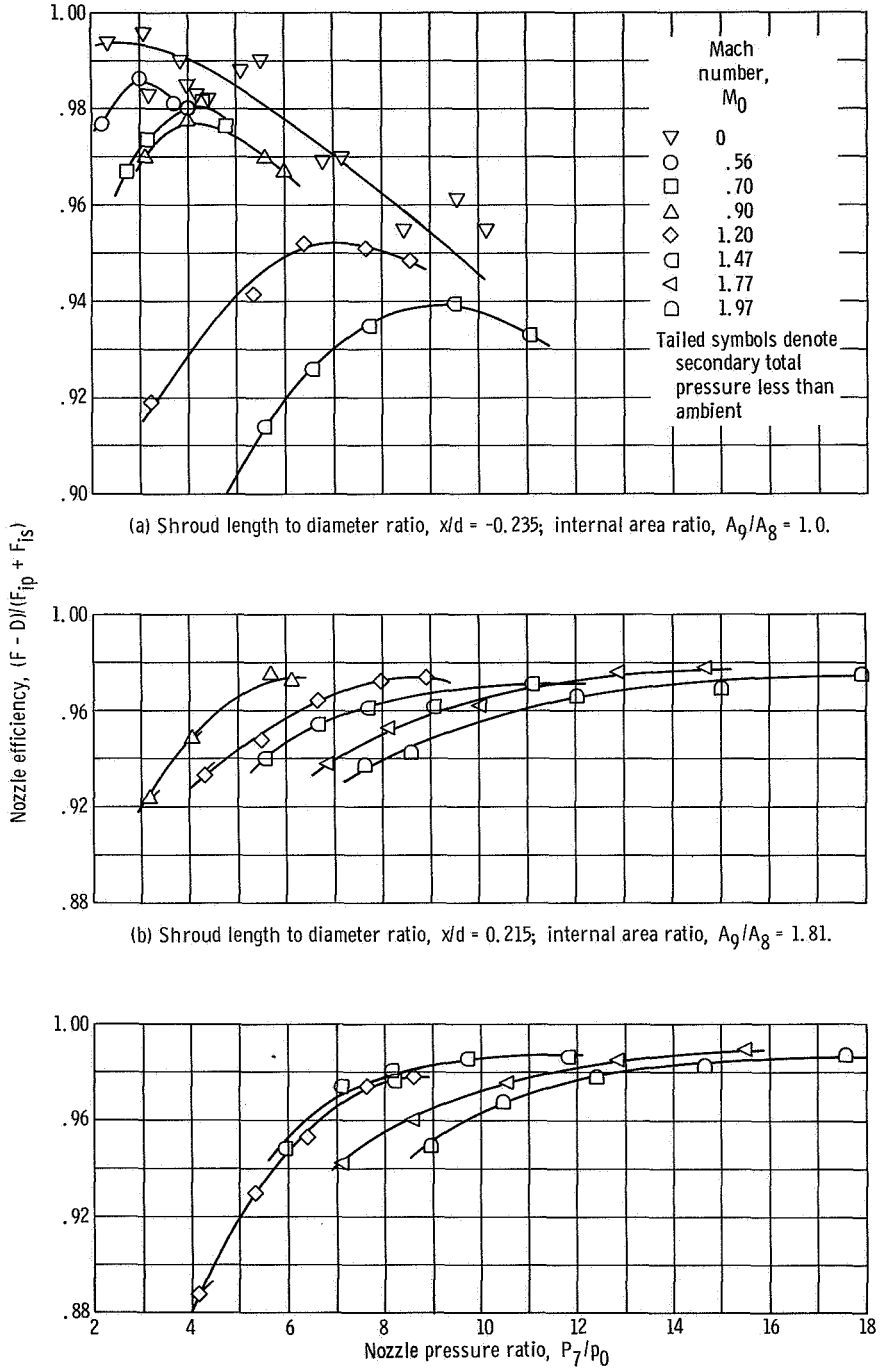

(a) Shroud length to diameter ratio, x/d = -0.235; internal area ratio, A_9/A_8 = 1.0.

(b) Shroud length to diameter ratio, x/d = 0.215; internal area ratio, A_9/A_8 = 1.81.

(c) Shroud length to diameter ratio, x/d = 0.618; internal area ratio, A_9/A_8 = 2.13.

Figure 11. - External flow effect on full-length plug nozzle performance; afterburner on; corrected secondary flow ratio, $(w_s/w_p)\sqrt{T_s/T_p}$ = 4 percent.

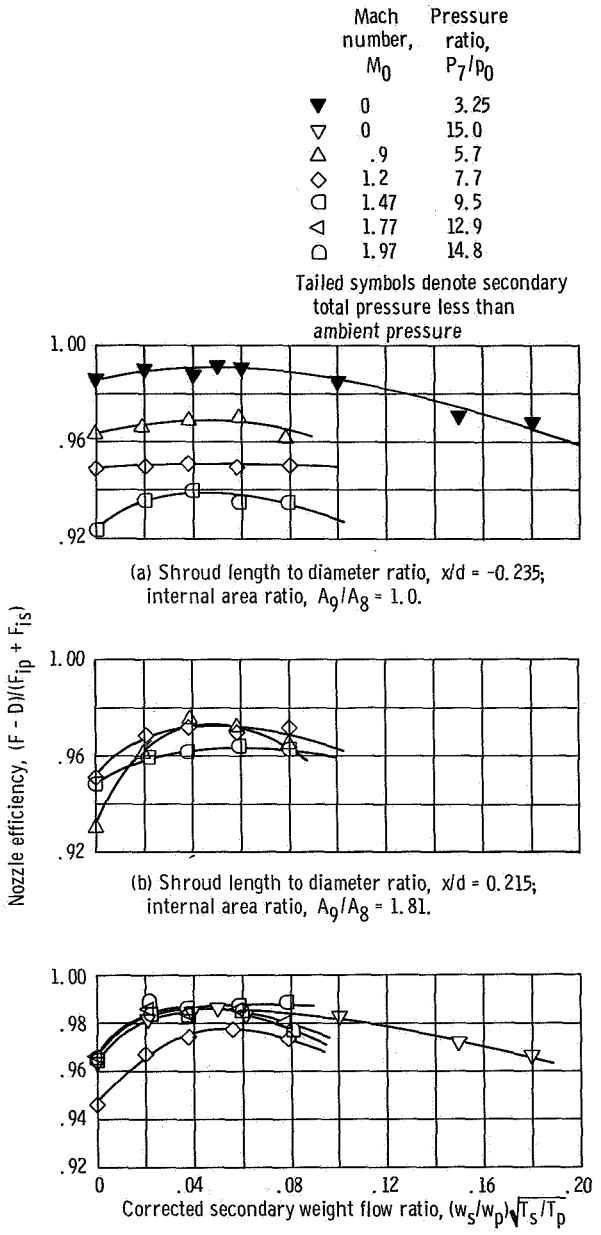

(a) Shroud length to diameter ratio, x/d = -0.235; internal area ratio, A_9/A_8 = 1.0.

(b) Shroud length to diameter ratio, x/d = 0.215; internal area ratio, A_9/A_8 = 1.81.

(c) Shroud length to diameter ratio, x/d = 0.618; internal area ratio, A_9/A_8 = 2.13.

Figure 12. - Effect of secondary flow on performance of full-length plug nozzle with afterburner on.

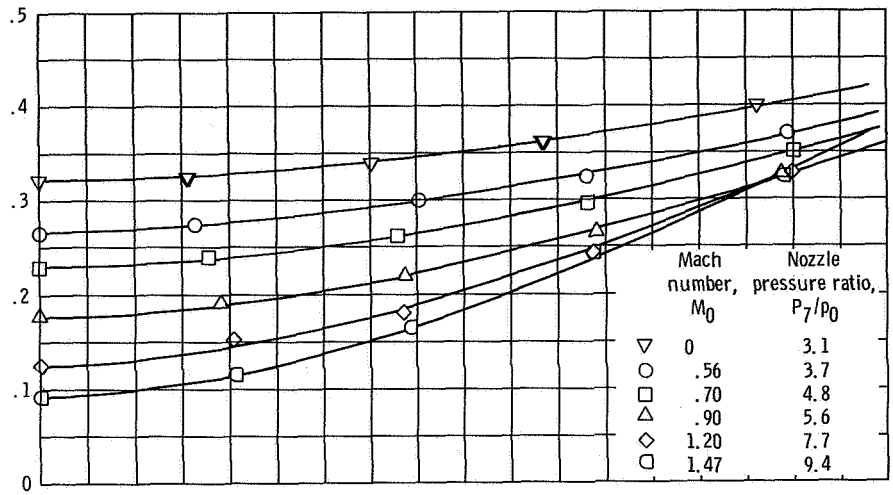

(a) Shroud length to diameter ratio, x/d = -0.235; internal area ratio, A_9/A_8 = 1.0.

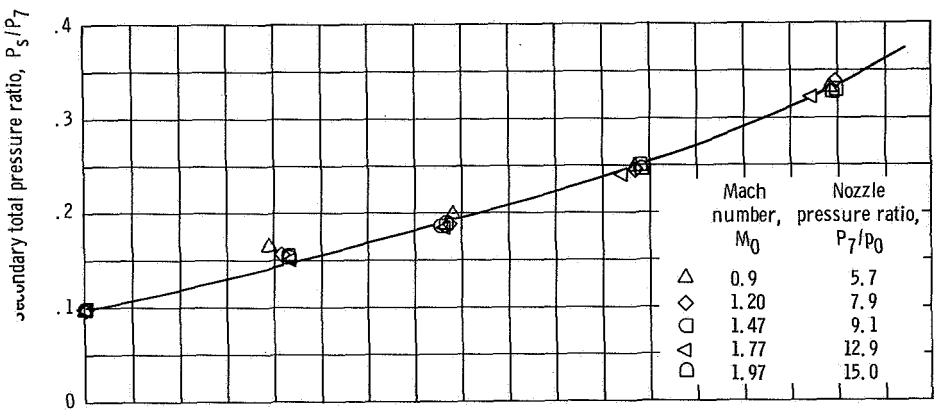

(b) Shroud length to diameter ratio, x/d = 0.215; internal area ratio, A_9/A_8 = 1.81.

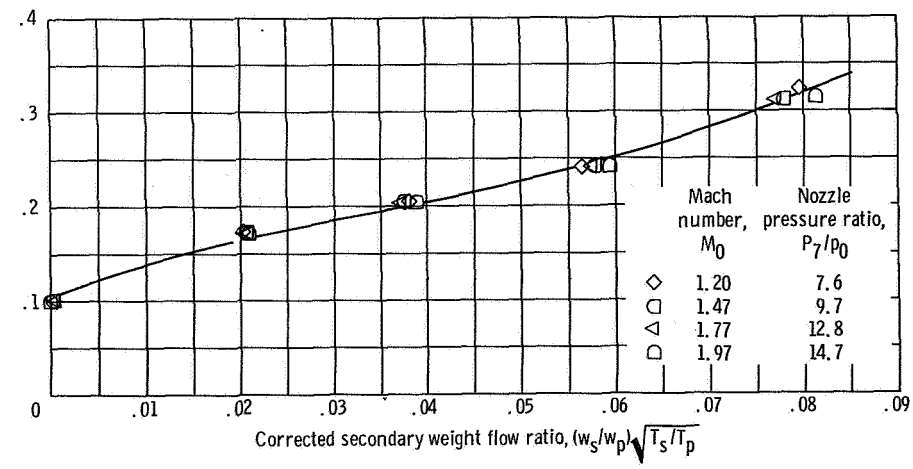

(c) Shroud length to diameter ratio, x/d = 0.618; internal area ratio, A_9/A_8 = 2.13.

Figure 13. - Pumping characteristic curves for afterburner on.

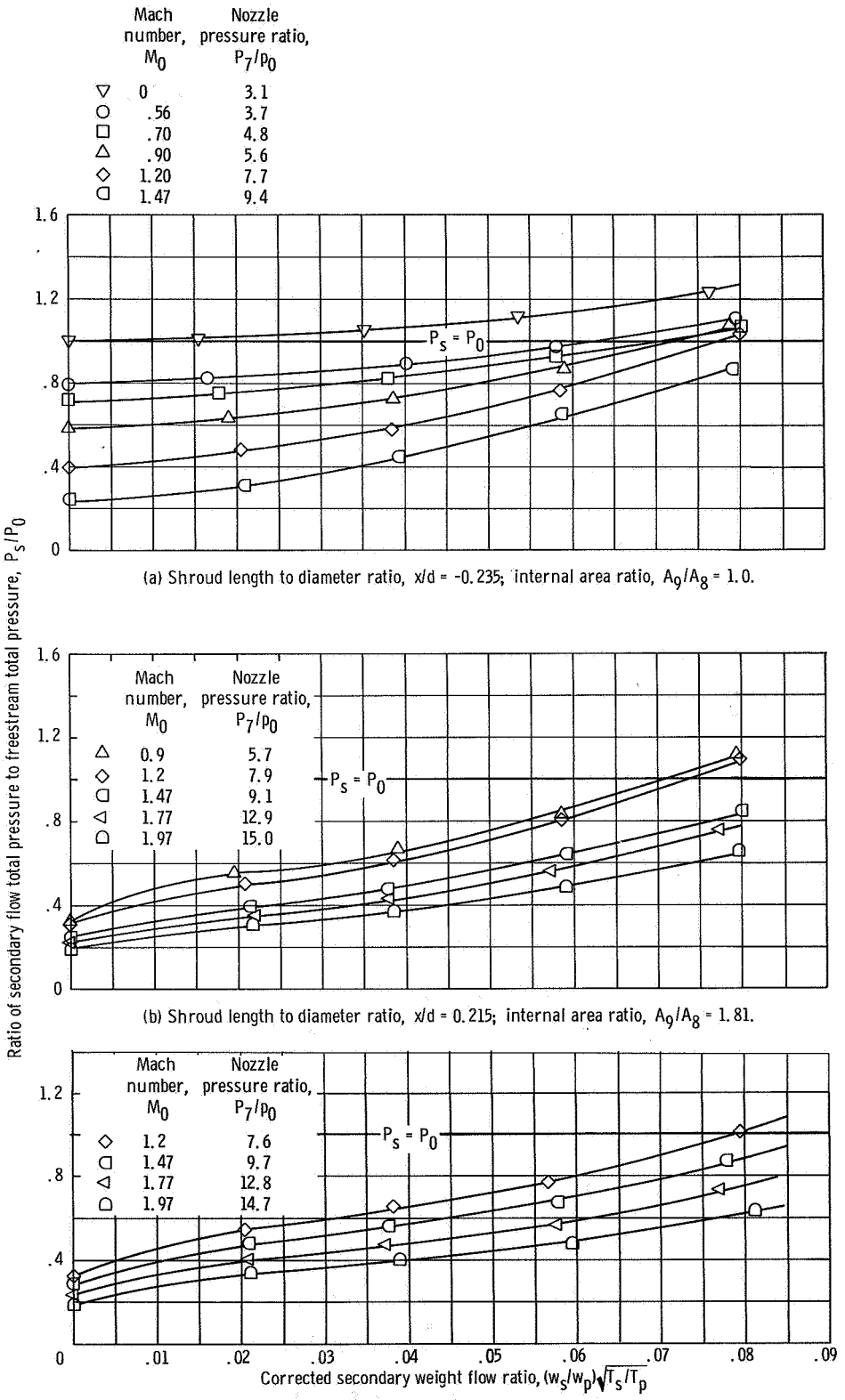

(a) Shroud length to diameter ratio, x/d = -0.235; internal area ratio, A_9/A_8 = 1.0.

(b) Shroud length to diameter ratio, x/d = 0.215; internal area ratio, A_9/A_8 = 1.81.

(c) Shroud length to diameter ratio, x/d = 0.618; internal area ratio, A_9/A_8 = 2.13.

Figure 14. - Secondary flow pressure recovery requirement for full-length plug nozzle with afterburner on.

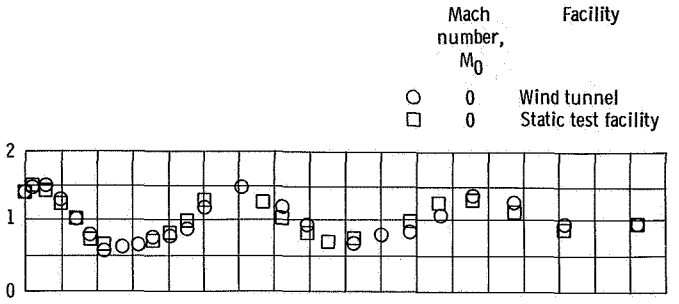

(a) Shroud length to diameter ratio, x/d = -0.235; internal area ratio, A_9/A_8 = 1.0; nozzle pressure ratio, P_7/p_0 = 3.10.

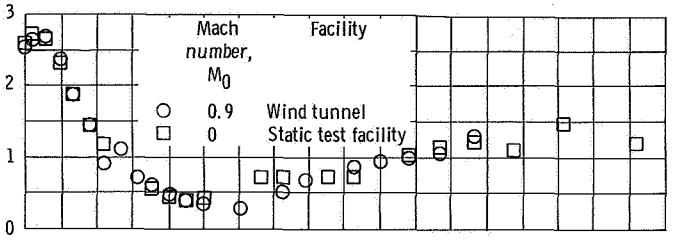

(b) Shroud length to diameter ratio, x/d = -0.235; internal area ratio, A_9/A_8 = 1.0; nozzle pressure ratio, P_7/p_0 = 5.65.

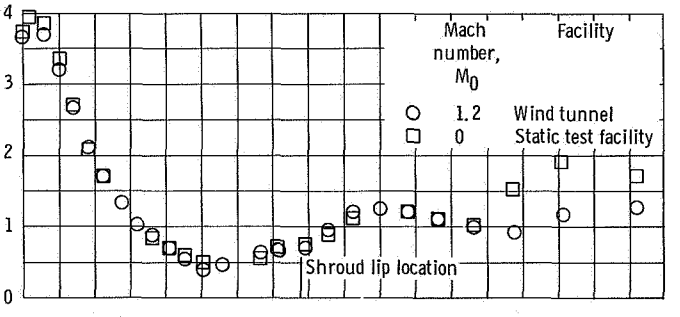

(c) Shroud length to diameter ratio, x/d = 0.618; internal area ratio, A_9/A_8 = 2.13; nozzle pressure ratio, P_7/p_0 = 7.9.

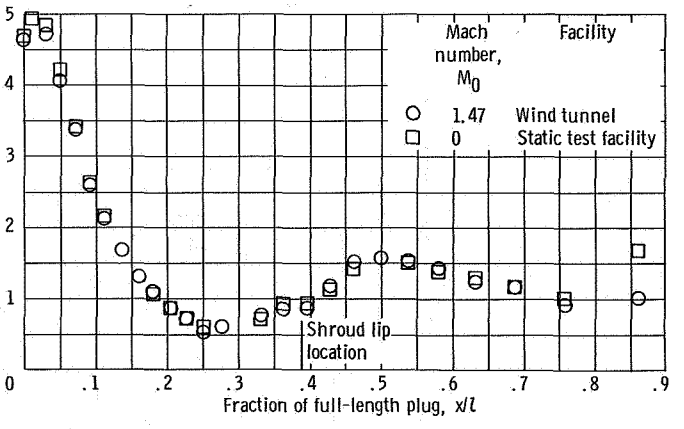

(d) Shroud length to diameter ratio, x/d = 0.618; internal area ratio, A_9/A_8 = 2.13; nozzle pressure ratio, P_7/p_0 = 10.0.

Figure 15. - Effect of external flow on plug pressure distribution. Afterburner on; corrected secondary flow ratio, $(w_s/w_p)\sqrt{T_s/T_p}$ = 0 percent.

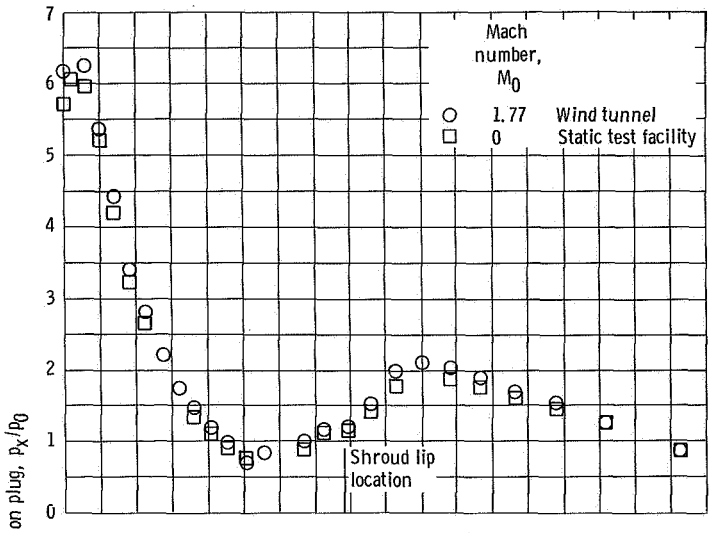

(e) Shroud length to diameter ratio, x/d = 0.618; internal area ratio, A_9/A_8 = 2.13; nozzle pressure ratio, P_7/p_0 = 12.75.

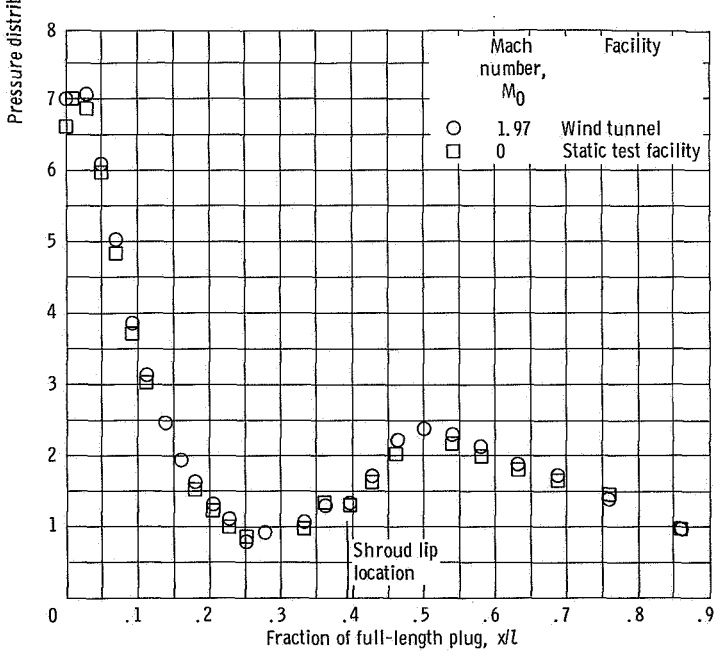

(f) Shroud length to diameter ratio, x/d = 0.618; internal area ratio, A_9/A_8 = 2.13; nozzle pressure ratio, P_7/p_0 = 14.60.

Figure 15. - Concluded.

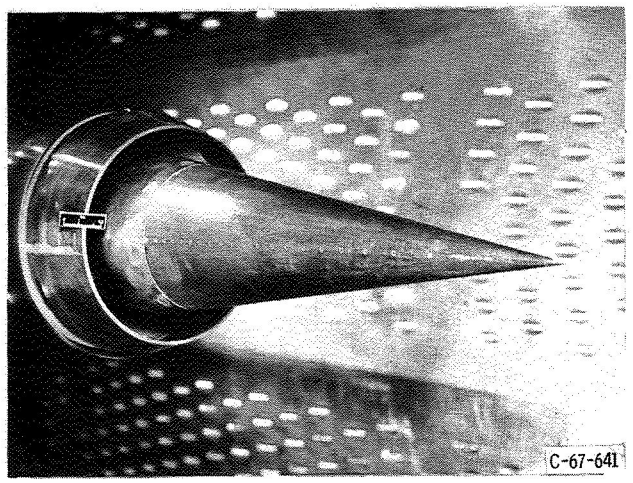

(a) Shroud length to diameter ratio, x/d = -0.235; internal area ratio, A_9/A_8 1.0.

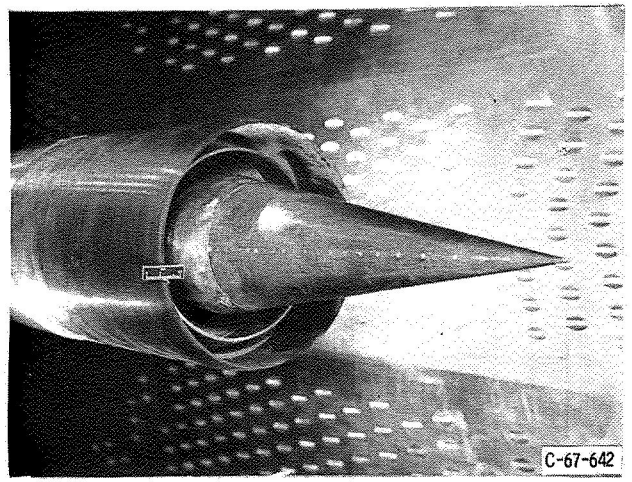

(b) Shroud length to diameter ratio, x/d = 0.215; internal area ratio, A_9/A_8 = 2.54.

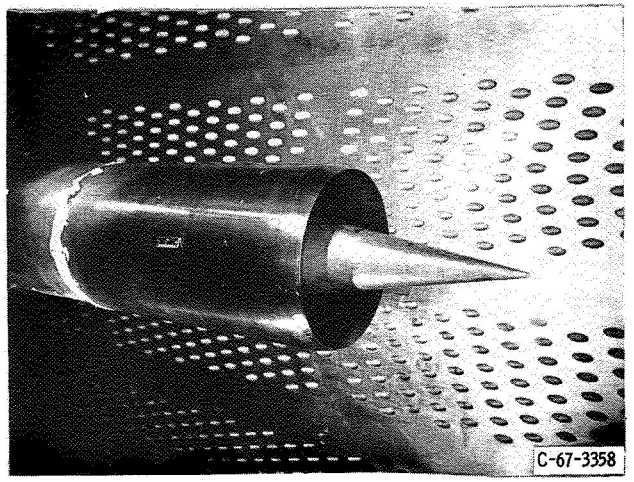

(c) Shroud length to diameter ratio, x/d = 0.618; internal area ratio, A_9/A_8 = 2.99.

Figure 16. - Full-length plug with translating shroud and afterburner off.

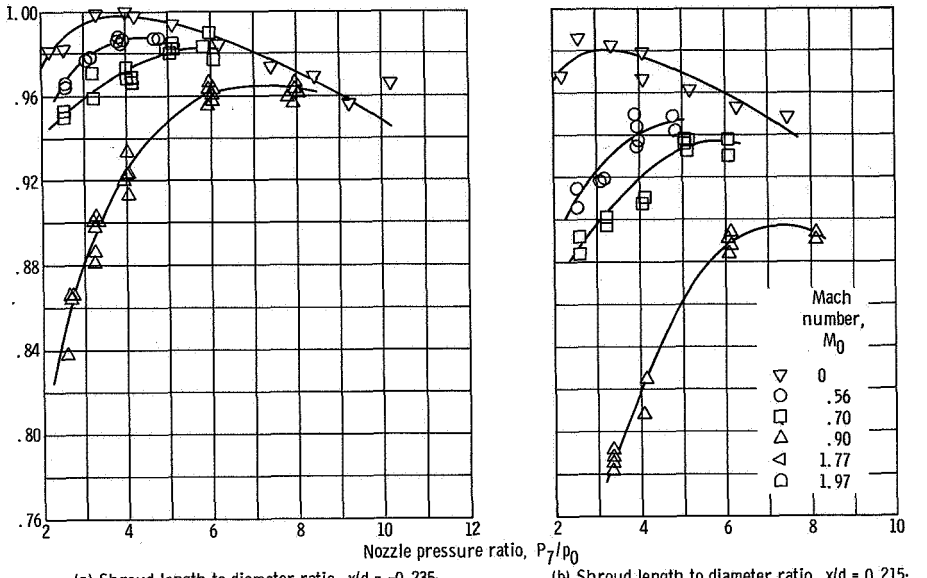

(a) Shroud length to diameter ratio, x/d = -0.235; internal area ratio, A_9/A_8 = 1.0.

(b) Shroud length to diameter ratio, x/d = 0.215; internal area ratio, A_9/A_8 = 2.54.

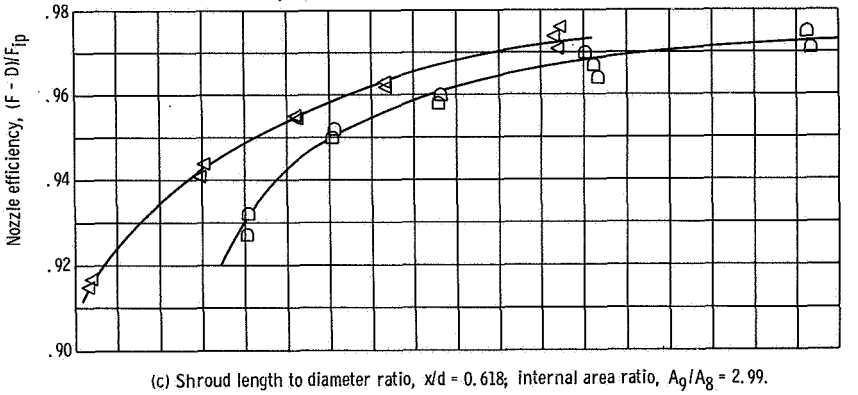

(c) Shroud length to diameter ratio, x/d = 0.618; internal area ratio, A_9/A_8 = 2.99.

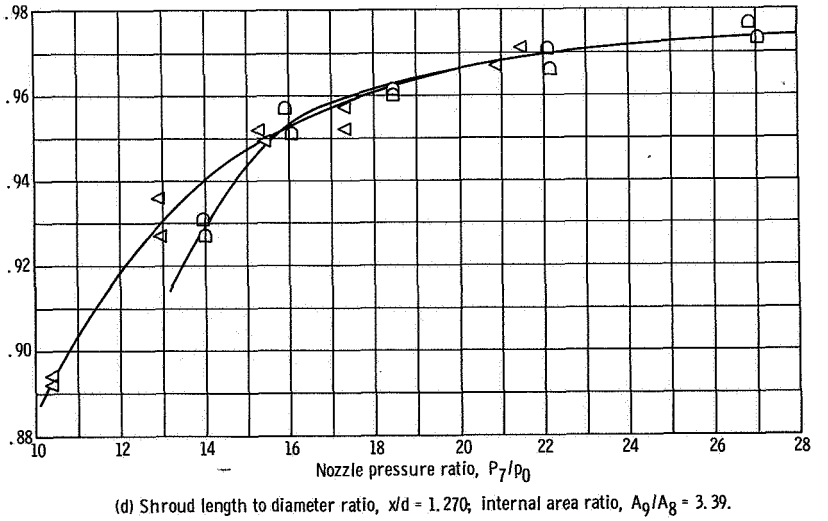

(d) Shroud length to diameter ratio, x/d = 1.270; internal area ratio, A_9/A_8 = 3.39.

Figure 17. - External flow effect on full-length plug nozzle performance. Afterburner off; corrected secondary flow ratio, $(w_s/w_p)\sqrt{T_s/T_p}$ = 0 percent.

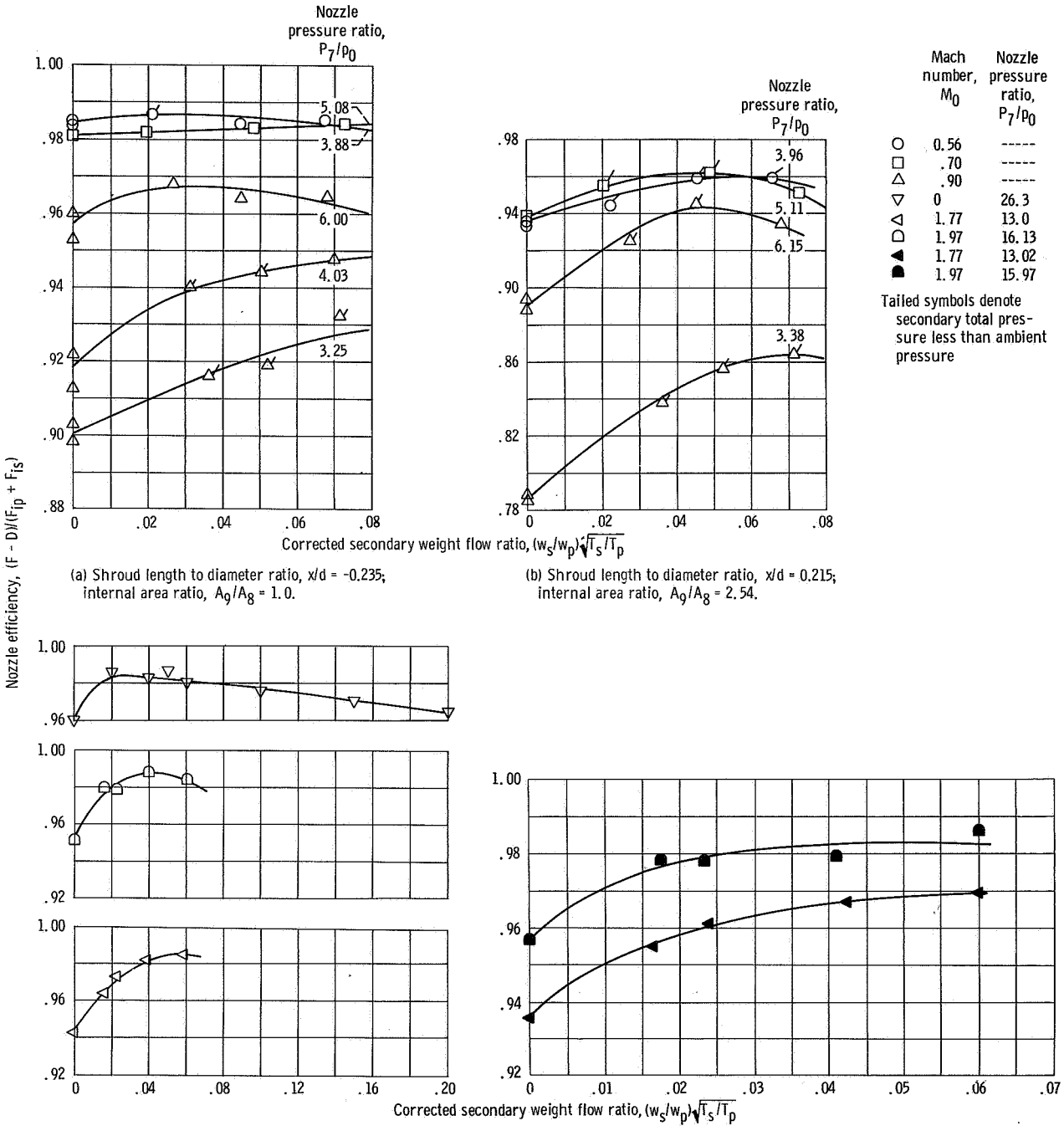

(a) Shroud length to diameter ratio, x/d = -0.235; internal area ratio, A_9/A_8 = 1.0.

(b) Shroud length to diameter ratio, x/d = 0.215; internal area ratio, A_9/A_8 = 2.54.

(c) Shroud length to diameter ratio, x/d = 0.618; internal area ratio, A_9/A_8 = 2.99.

(d) Shroud length to diameter ratio, x/d = 1.270; internal area ratio, A_9/A_8 = 3.39.

Figure 18. - Effect of secondary flow on performance of full-length plug nozzle with afterburner off.

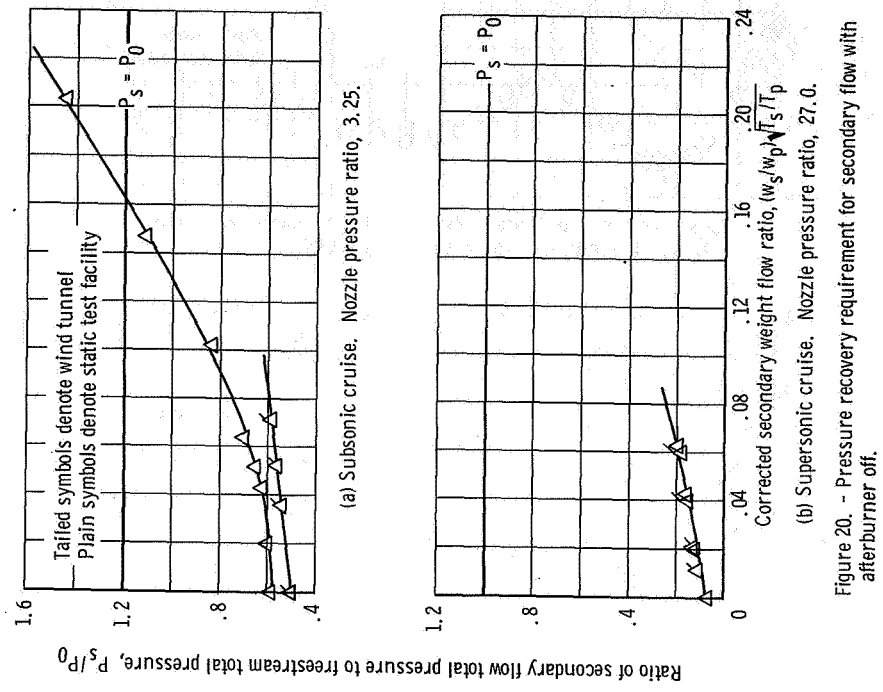

Figure 20. - Pressure recovery requirement for secondary flow with afterburner off.

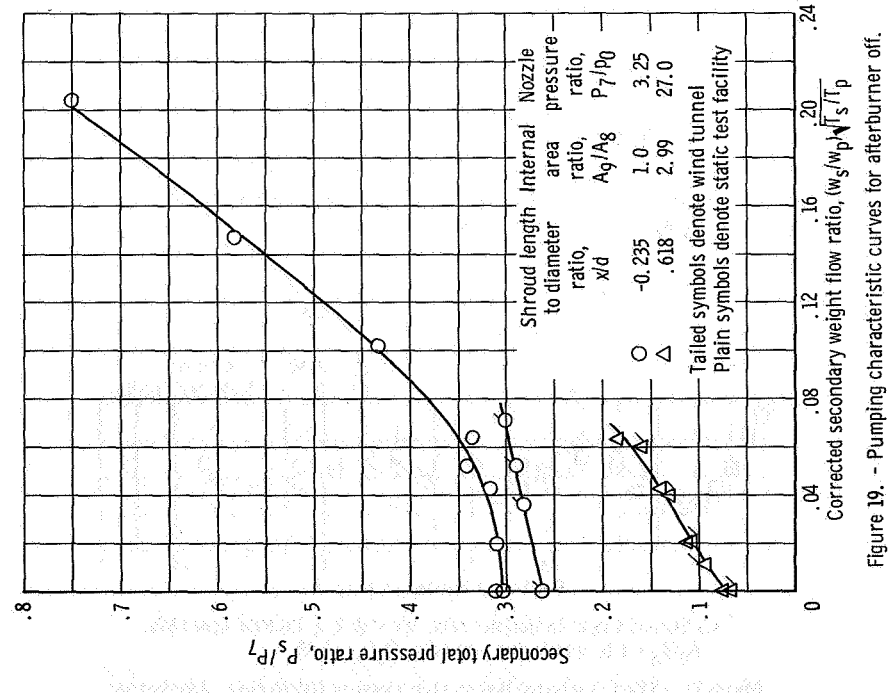

Figure 19. - Pumping characteristic curves for afterburner off.

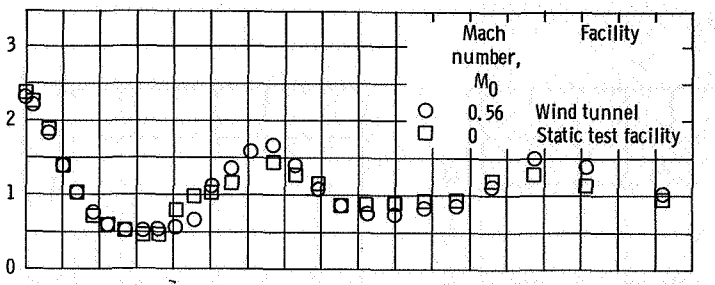

(a) Shroud length to diameter ratio, x/d = -0.235; internal area ratio, A_9/A_8 = 1.0; nozzle pressure ratio, P_7/p_0 = 3.95.

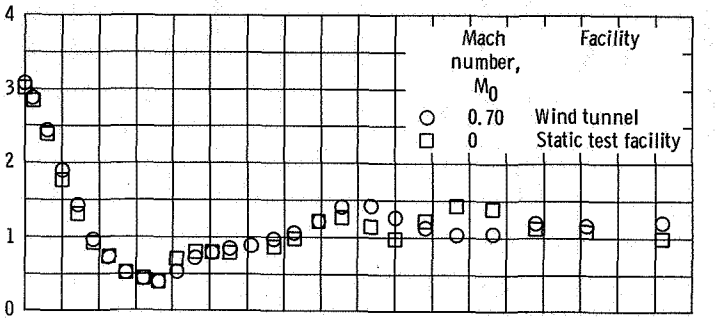

(b) Shroud length to diameter ratio, x/d = -0.235; internal area ratio, A_9/A_8 = 1.0; nozzle pressure ratio, P_7/p_0 = 5.10.

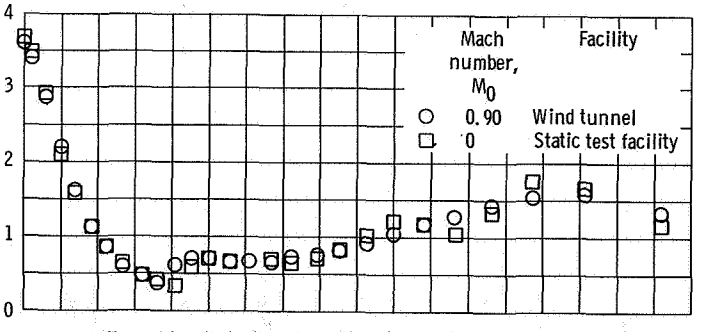

(c) Shroud length to diameter ratio, x/d = -0.235; internal area ratio, A_9/A_8 = 1.0; nozzle pressure ratio, P_7/p_0 = 6.12.

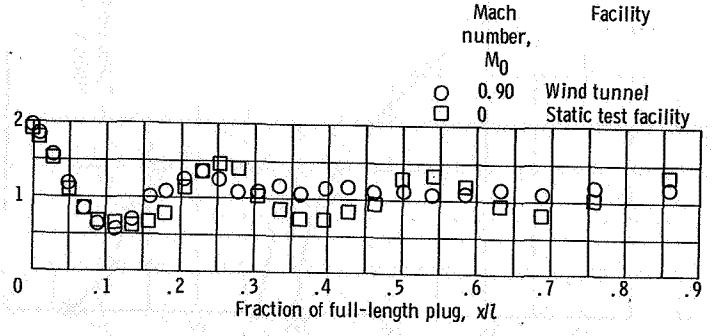

(d) Shroud length to diameter ratio, x/d = -0.235; internal area ratio, A_9/A_8 = 1.0; nozzle pressure ratio, P_7/p_0 = 3.25.

Figure 21. - Effect of external flow on plug pressure distribution. Afterburner off; corrected secondary flow ratio, $(w_s/w_p)\sqrt{T_s/T_p}$ = 0 percent.

Pressure distribution on plug, p_x/p_0

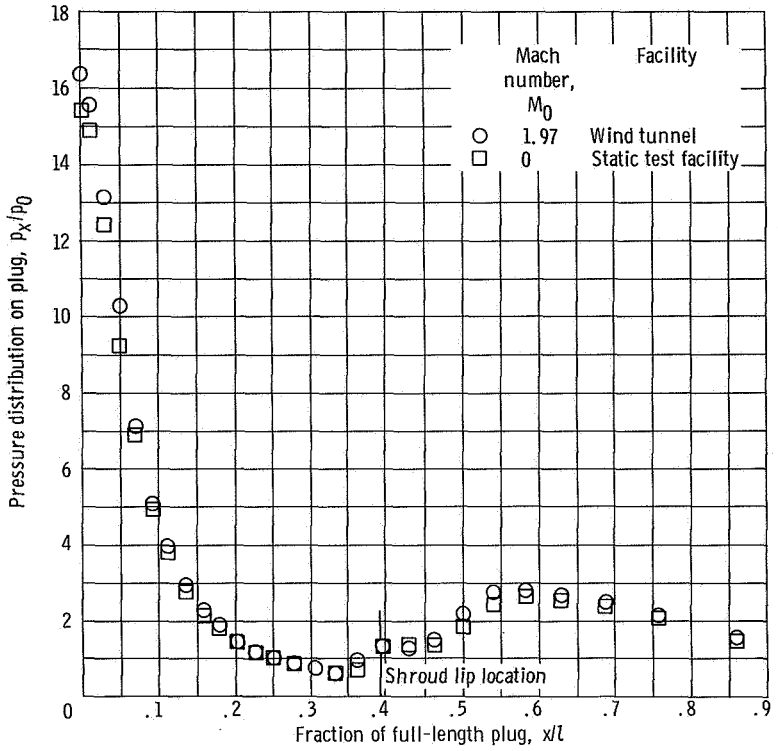

(e) Shroud length to diameter ratio, x/d = 0.618; internal area ratio, A_9/A_8 = 2.99; nozzle pressure ratio, P_7/p_0 = 27.2.

Figure 21. - Concluded.

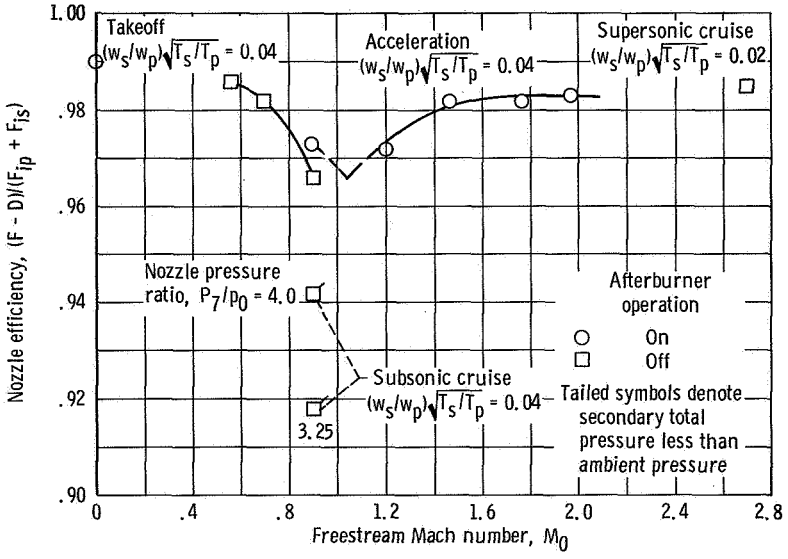

Figure 22. - Nozzle performance over flight Mach number range.

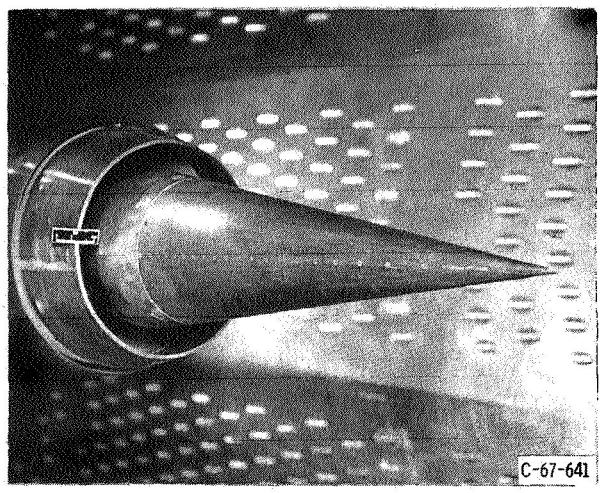

(a) Plug length, 100 percent.

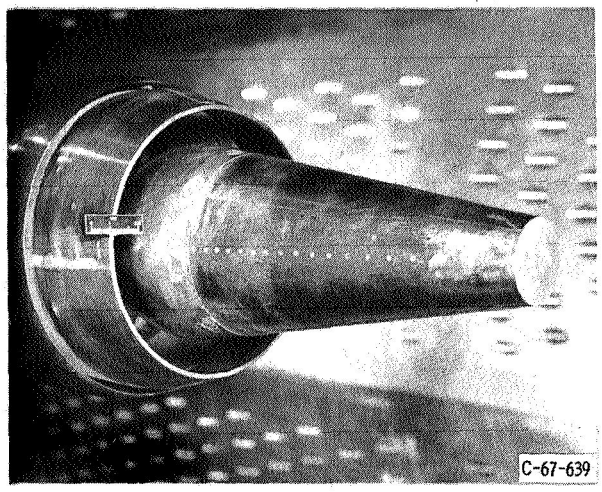

(b) Plug length, 65 percent.

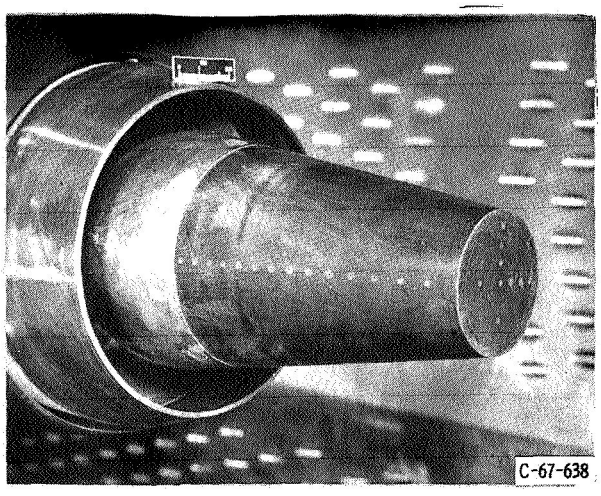

(c) Plug length, 50 percent.

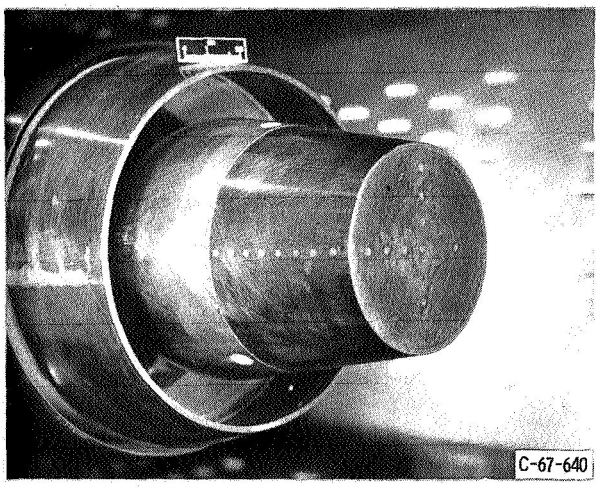

(d) Plug length, 30 percent.

Figure 23. - Truncated plugs with fully retracted shroud.

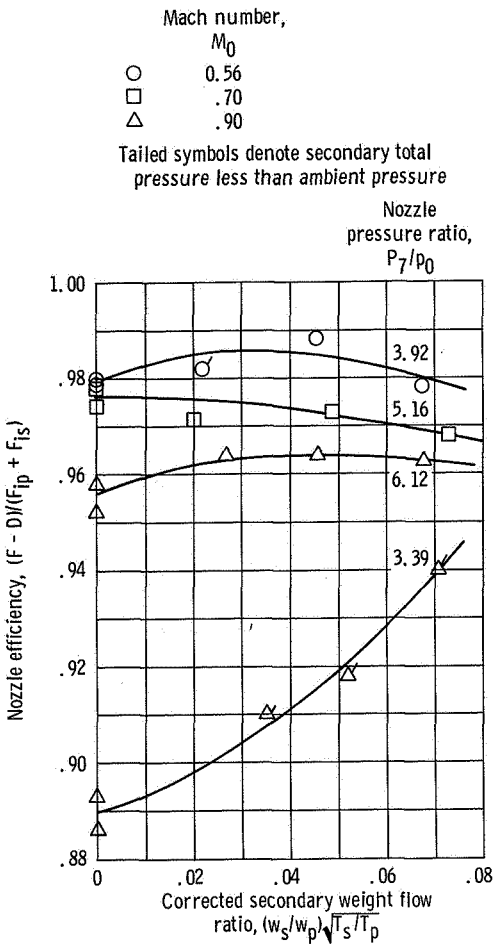

Figure 25. - Effect of secondary flow on performance of a 65-percent plug nozzle. Afterburner off; shroud length to diameter ratio, x/d = -0.235; internal area ratio, A_9/A_8 = 1.0.

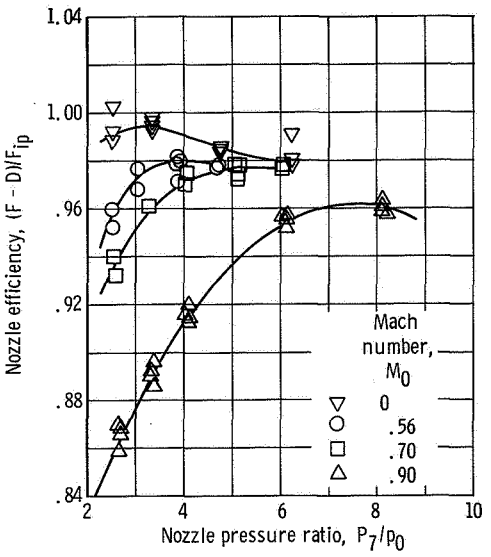

Figure 24. - External flow effect on 65-percent plug nozzle performance. Afterburner off; corrected secondary flow ratio, $(w_s/w_p)\sqrt{T_s/T_p}$ = 0 percent; shroud length to diameter ratio, x/d = -0.235; internal area ratio, A_9/A_8 = 1.0.

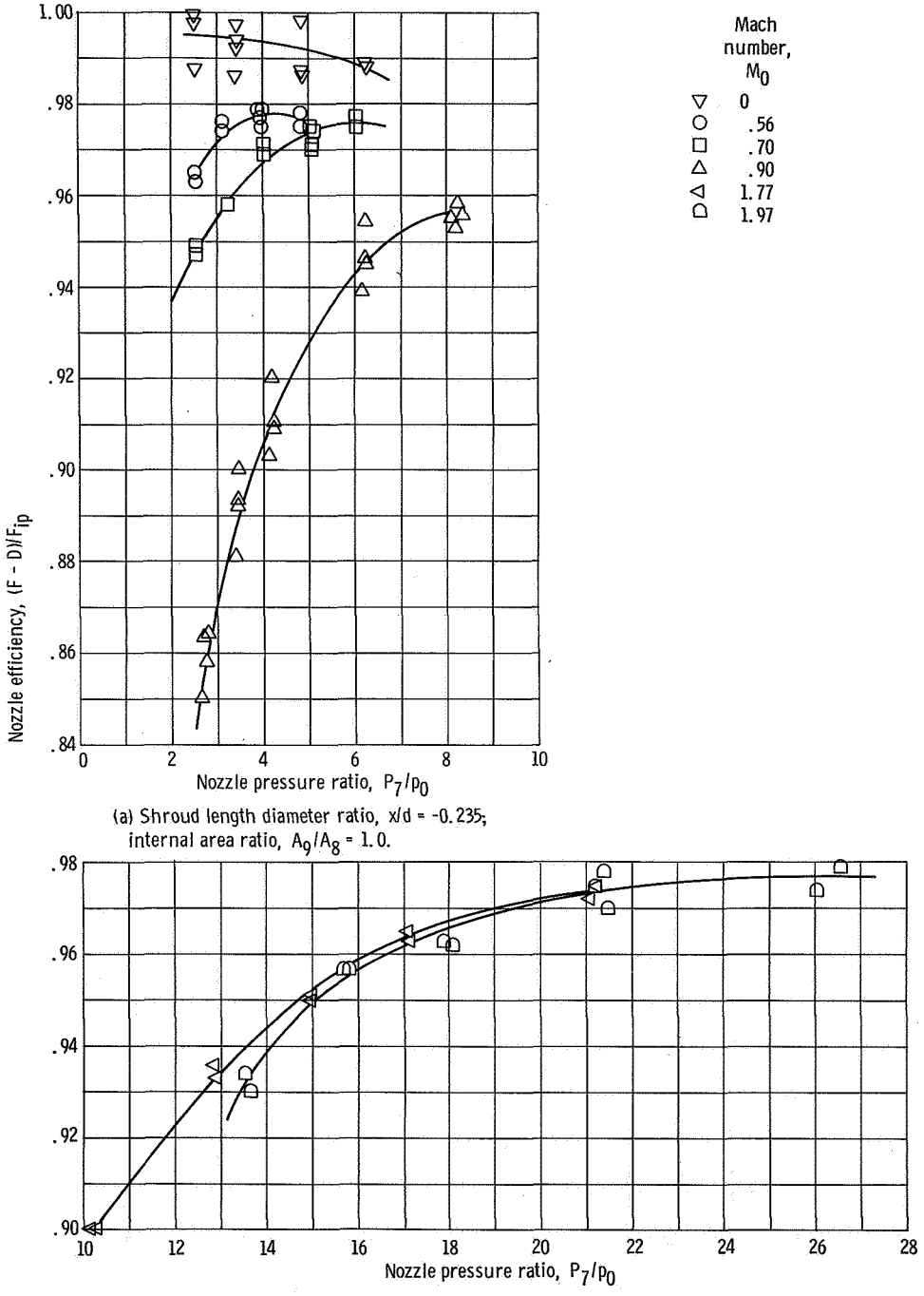

(a) Shroud length diameter ratio, x/d = -0.235; internal area ratio, A_9/A_8 = 1.0.

(b) Shroud length to diameter ratio, x/d = 0.618; internal area ratio, A_9/A_8 = 2.99.

Figure 26. - External flow effect on 50-percent plug nozzle performance. Afterburner off; corrected secondary flow ratio, $(w_s/w_p)\sqrt{T_s/T_p}$ = 0 percent.

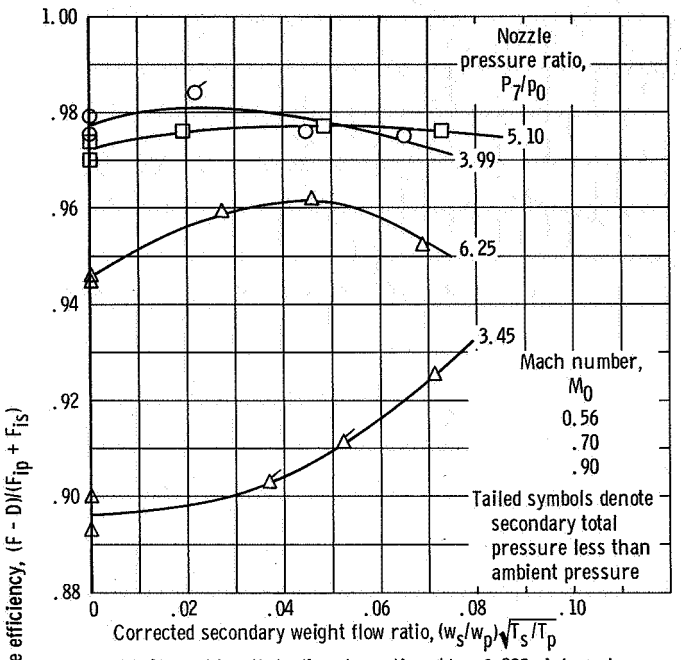

(a) Shroud length to diameter ratio, x/d = -0.235; internal area ratio, A_9/A_8 = 1.0.

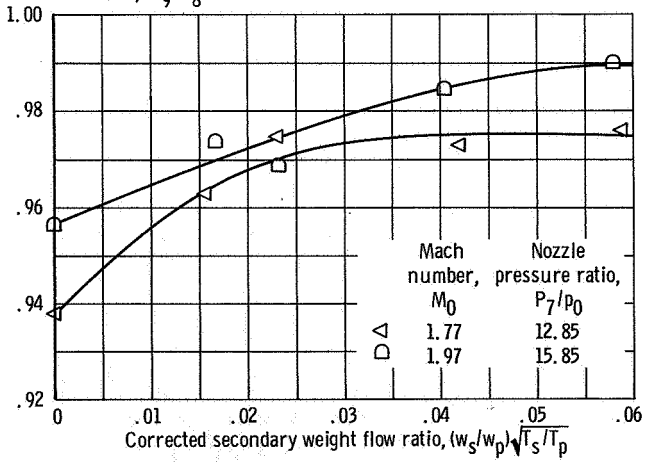

(b) Shroud length to diameter ratio, x/d = 0.618; internal area ratio, A_9/A_8 = 2.99.

Figure 27. - Effect of secondary flow on performance of a 50-percent plug nozzle with afterburner off.

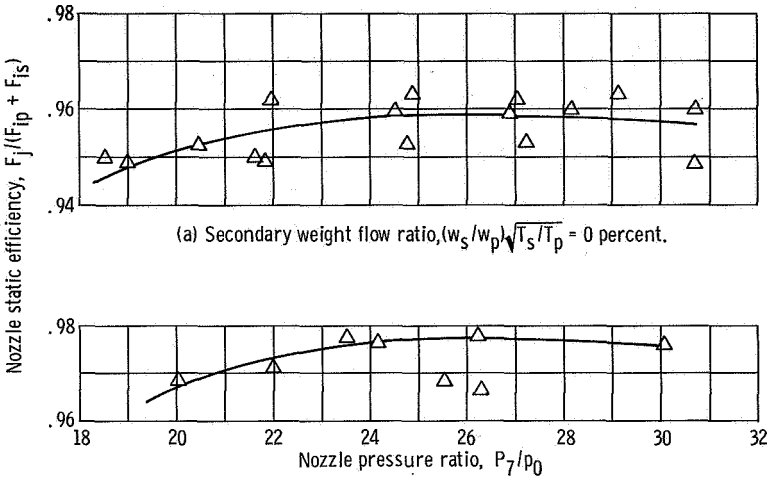

Figure 28. - Static performance of a 50-percent plug nozzle with afterburner off. Shroud length to diameter ratio, x/d = 0.618; internal area ratio, A_9/A_8 = 2.99.

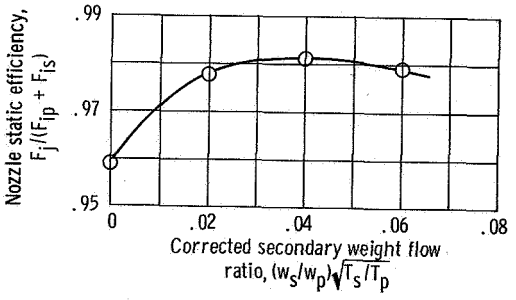

Figure 29. - Effect of secondary flow on performance of 50-percent plug nozzle. Afterburner off; shroud length to diameter ratio, x/d = 0.618; internal area ratio, A_9/A_8 = 2.99; nozzle pressure ratio, P_7/p_0 = 26.3.

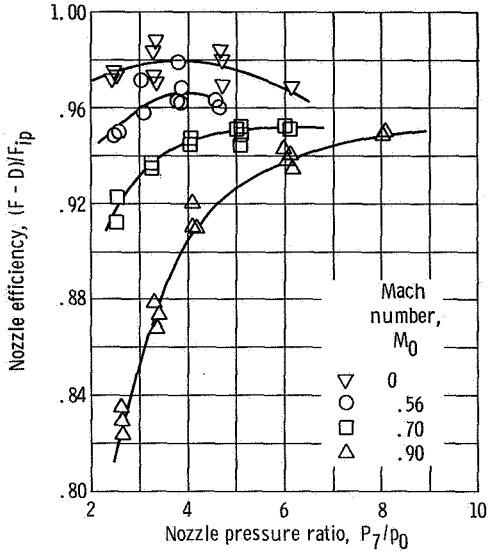

Figure 30. - External flow effect on 30-percent plug nozzle performance. Afterburner off; corrected secondary flow ratio, $(w_s/w_p)\sqrt{T_s/T_p}$ = 0 percent; shroud length to diameter ratio, x/d = -0.235; internal area ratio, A_9/A_8 = 1.0.

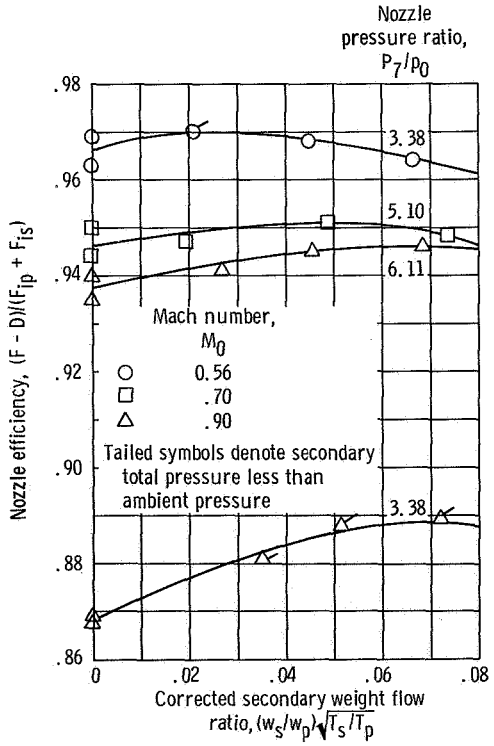

Figure 31. - Effect of secondary flow on performance of 30-percent plug nozzle. Afterburner off; shroud length to diameter ratio, x/d = -0.235; internal area ratio, A_9/A_8 = 1.0.

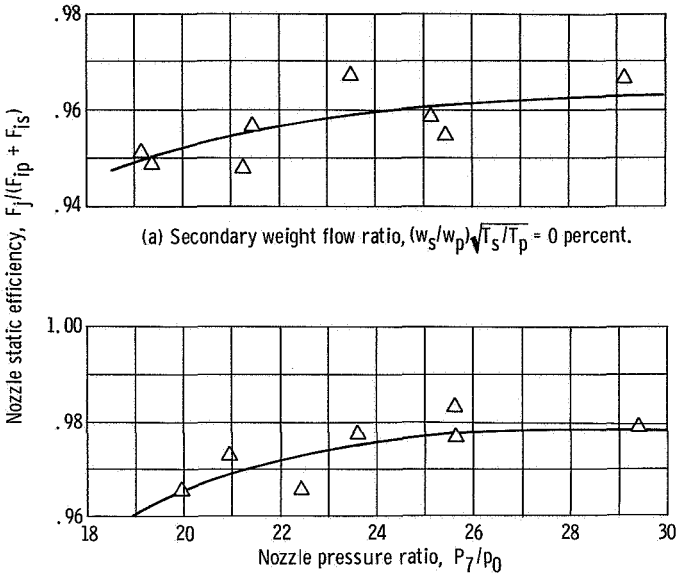

(a) Secondary weight flow ratio, $(w_s/w_p)\sqrt{T_s/T_p}$ = 0 percent.

(b) Corrected secondary weight flow ratio, $(w_s/w_p)\sqrt{T_s/T_p}$ = 2 percent.

Figure 32. - Static performance of a 30-percent plug nozzle with afterburner off.

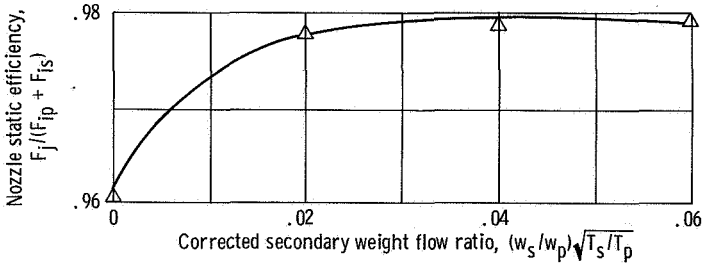

Figure 33. - Effect of secondary flow on performance of 30-percent plug nozzle. Afterburner off; shroud length to diameter ratio, x/d = 0.618; internal area ratio, A_9/A_8 = 2.99; nozzle pressure ratio, P_7/p_0 = 26.0.

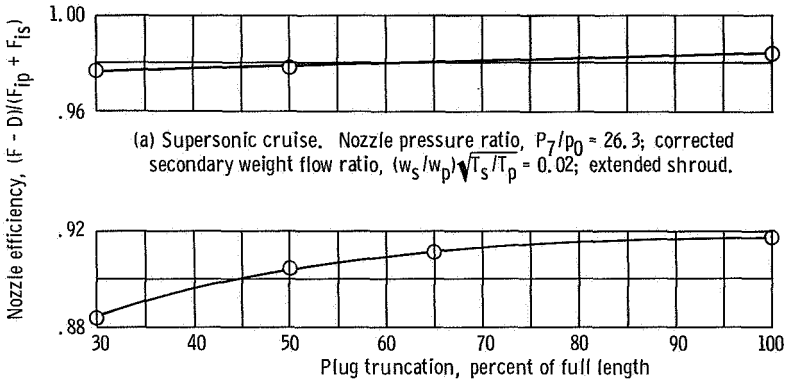

(a) Supersonic cruise. Nozzle pressure ratio, $P_7/p_0 = 26.3$; corrected secondary weight flow ratio, $(w_s/w_p)\sqrt{T_s/T_p} = 0.02$; extended shroud.

(b) Subsonic cruise. Nozzle pressure ratio, $P_7/p_0 = 3.25$; corrected secondary weight flow ratio, $(w_s/w_p)\sqrt{T_s/T_p} = 0.04$; free stream Mach number, $M_0 = 0.9$; retracted shroud.

Figure 34. - Effect of plug truncation on nozzle performance.

NATIONAL AERONAUTICS AND SPACE ADMINISTRATION
WASHINGTON, D. C. 20546

OFFICIAL BUSINESS

FIRST CLASS MAIL

POSTAGE AND FEES PAI
NATIONAL AERONAUTICS
SPACE ADMINISTRATION

POSTMASTER: If Undeliverable (Section
Postal Manual) Do Not R

"The aeronautical and space activities of the United States shall be conducted so as to contribute . . . to the expansion of human knowledge of phenomena in the atmosphere and space. The Administration shall provide for the widest practicable and appropriate dissemination of information concerning its activities and the results thereof."

—NATIONAL AERONAUTICS AND SPACE ACT OF 1958

NASA SCIENTIFIC AND TECHNICAL PUBLICATIONS

TECHNICAL REPORTS: Scientific and technical information considered important, complete, and a lasting contribution to existing knowledge.

TECHNICAL NOTES: Information less broad in scope but nevertheless of importance as a contribution to existing knowledge.

TECHNICAL MEMORANDUMS: Information receiving limited distribution because of preliminary data, security classification, or other reasons.

CONTRACTOR REPORTS: Scientific and technical information generated under a NASA contract or grant and considered an important contribution to existing knowledge.

TECHNICAL TRANSLATIONS: Information published in a foreign language considered to merit NASA distribution in English.

SPECIAL PUBLICATIONS: Information derived from or of value to NASA activities. Publications include conference proceedings, monographs, data compilations, handbooks, sourcebooks, and special bibliographies.

TECHNOLOGY UTILIZATION PUBLICATIONS: Information on technology used by NASA that may be of particular interest in commercial and other non-aerospace applications. Publications include Tech Briefs, Technology Utilization Reports and Notes, and Technology Surveys.

Details on the availability of these publications may be obtained from:

SCIENTIFIC AND TECHNICAL INFORMATION DIVISION

NATIONAL AERONAUTICS AND SPACE ADMINISTRATION

Washington, D.C. 20546